ORIGINAL ARTICLE

Drought tolerance differs between urban tree species but is not affected by the intensity of traffic pollution

Mareike Hirsch[1,2] · Helena Böddeker[1] · Axel Albrecht[1] · Somidh Saha[3,4]

Abstract

Key Message In an urban area, resistance and resilience of stem diameter growth differ substantially between tree species. Traffic emissions are reflected in wood nitrogen isotopes, but do not affect drought tolerance.

Abstract With increasing drought and heat, the benefits of urban trees such as shading and cooling become more important. Yet, it is necessary to identify tree species able to withstand such extreme climatic conditions. We studied the resistance and resilience of stem diameter growth of five deciduous tree species in an urban area in Southwest Germany to three exceptional drought periods (2003, 2011 and 2015) for differences between and within species, especially considering the intensity of traffic emissions (NO_x). Analyses of the stable isotopic composition of carbon ($\delta^{13}C$) and oxygen ($\delta^{18}O$) as well as the intrinsic water-use efficiency (WUE_i) in the tree rings were carried out. Further, we investigated the stable isotopic composition of nitrogen in the wood ($\delta^{15}N$) to assess its potential as an indicator of NO_x emissions from traffic. Stem diameter growth in all species was strongly limited by low water availability in spring, as was also reflected in elevated $\delta^{13}C$ and $\delta^{18}O$ values in *Acer platanoides* and *Tilia cordata*, which were particularly sensitive to drought. In contrast, growth of *Platanus × hispanica* and *Quercus robur* was less affected by drought, and resistance of *Carpinus betulus* ranged in between. Across species, $\delta^{15}N$ was higher in trees located closer to roads and exposed to higher NO_x traffic emissions. Unexpectedly, these conditions did not significantly affect drought resistance/resilience. Our study demonstrates the potential and interpretative challenges of coupled dendroecological and isotope analyses. It also indicates clear species-specific differences in drought tolerance and thus helps to identify suitable urban tree species.

Keywords Stable isotope analysis · Dendroecology · Resistance · Resilience · Suitability

✉ Mareike Hirsch
mareike.hirsch@iww.uni-freiburg.de

1 Forest Research Institute Baden-Wuerttemberg (FVA), Wonnhaldestr. 4, 79100 Freiburg, Germany

2 Chair of Forest Growth and Dendroecology, Institute of Forest Sciences, University of Freiburg, Tennenbacher Str. 4, 79106 Freiburg, Germany

3 Institute for Technology Assessment and Systems Analysis (ITAS), Karlsruhe Institute of Technology, Karlstr.11, 76133 Karlsruhe, Germany

4 Chair of Silviculture, Institute of Forest Sciences, University of Freiburg, Tennenbacher Str. 4, 79106 Freiburg, Germany

Introduction

Trees in urban areas provide a multitude of services (Dümpelmann 2020); They contribute to the reduction of air pollution as gaseous pollutants are taken up as an effect of stomatal conductance and particles are deposited to the surface of the leaves and bark (Maher et al. 2013; Hofman et al. 2014; Grote et al. 2016; Pace et al. 2020). A simulation study carried out in the city of London showed that, while solid barriers such as low boundary walls can drastically reduce NO_2 concentrations on the sidewalk, trees are the most cost-effective measure to mitigate pollution (Jeanjean et al. 2017). Trees also provide further benefits. Especially on warm summer days, the temperature below the canopy remains substantially lower than above exposed concrete surroundings, as the trees provide shading and a further cooling effect due to transpiration (Pace et al. 2020; Sanusi and Livesley 2020). Trees in urban areas also store significant amounts

of carbon—especially (old) trees in parks and cemeteries contribute to carbon storage (Kändler et al. 2011; Strohbach and Haase 2012; Richter et al. 2020).

At the same time, air pollution and its filtering by trees may also affect tree growth negatively (Locosselli et al. 2019). Here, assessing the stable isotopic composition of nitrogen in the wood ($\delta^{15}N$) can be useful to find out the degree of traffic pollution urban trees experience. Trees utilise nitrogen for different purposes such as (xylem) growth and also store it in the stem wood (Cowling and Merrill 1966; Millard and Grelet 2010), so that $\delta^{15}N$ of the wood reflects the isotopic composition of the nitrogen which is taken up from the soil. While isotope analyses of nitrogen oxide (NO_x) in vehicle exhaust and air close to a highway generally revealed a considerable variation of $\delta^{15}N$, values are mostly positive (Ammann et al. 1999; Felix and Elliott 2014) and thus higher than those of agricultural or natural sources (Beyn et al. 2014; Felix and Elliott 2014). Accordingly, $\delta^{15}N$ has been found to be higher in trees closer to a highway (Saurer et al. 2004; Guerrieri et al. 2009), but studies for trees in urban areas are lacking. Besides air pollution, urban trees are also exposed to soil compaction and soil contamination with heavy metals (Czaja et al. 2020), and the use of de-icing salt in winter can increase soil salinity and induce leaf damage (Dmuchowski et al. 2020, 2021) or reduced stem diameter growth (Helama et al. 2020).

However, trees can only provide the services mentioned above if they are vital. For instance, the cooling effect of roadside *Platanus × hispanica* trees diminished during a heat wave, and as the trees shed up to 50 % of their leaves in response to this period of high temperatures and low water availability, the positive effect on the microclimate was reduced for several weeks, even though overall the conditions remained cooler compared to open areas (Sanusi and Livesley 2020). For seedlings of *Tilia cordata* subjected to a drought-stress experiment, a model simulation showed substantially lower CO_2 fixation, evapotranspiration and cooling than for control trees (Zhang et al. 2019). If stomatal conductance declines or ceases entirely, this also reduces the removal of gaseous air pollution (Pace et al. 2020).

Based on climate modeling, the frequency, duration and intensity of heat waves will increase substantially in Southern Germany within this century (Zacharias et al. 2014), concomitant with a tentatively projected decrease of precipitation in the vegetation period and an increase in the duration of dry periods (LUBW 2013). Therefore, there has been an increase in not only the importance of vital trees in urban areas providing a beneficial microclimate, but also the necessity to identify tree species which may cope with increasingly hot and dry conditions.

In the city of Munich, the daily stem diameter growth of *Tilia cordata* trees was negatively correlated with vapour pressure deficit in the hot and dry summer months of the year 2015. The growth of trees at a paved site was impaired more than that of trees on an open green square, indicating that site conditions may either support or impede tree growth during drought periods (Moser et al. 2017). Water availability has also been determined a substantial influence on stem diameter growth for several tree species in the city of Dresden, where *Platanus × hispanica* and *Quercus* spp. were concluded to be more suitable in urban environments experiencing hot and dry conditions than *Acer* spp. (Gillner et al. 2014). There, *Platanus × hispanica* and *Quercus rubra* showed higher mean water-use efficiency than trees of the genera *Acer* and *Tilia* (Gillner et al. 2015), indicating that different water-use strategies may be the key to interspecific differences in drought tolerance (Gillner et al. 2016).

While tree ring series provide an extensive base for retrospective analyses of the influence of climatic conditions on tree growth, the informative value of comparing tree ring widths is slightly constrained. As stem diameter growth is of lower priority compared to other (growth) processes (Waring 1987; Dobbertin 2005), narrow tree rings do not necessarily imply poor vitality. Rather, the (temporal) competition of resources may have led to them being allocated to other compartments, e. g. for fructification in species, which exhibit pronounced masting patterns (Mund et al. 2010; Müller-Haubold et al. 2013). This may however not imply a long-term growth inhibition. Thus, to support the interpretation of the analysis of tree ring widths with regard to drought tolerance, the inter-annual variability in the stable isotopic composition of carbon and oxygen in the stem wood can give additional information on tree physiological processes (Gessler et al. 2018).

The isotopic composition of carbon is strongly influenced by the relation between stomatal conductance and photosynthesis, and increased $\delta^{13}C$ values indicate that trees may have experienced atmospheric and/or edaphic drought that led to reduced stomatal conductance (McCarroll and Loader 2004). However, an increase of $\delta^{13}C$ in the leaf can also be due to an increase in photosynthetic capacity at a constant stomatal conductance rate, so that the combined analysis of the variation of $\delta^{13}C$ and $\delta^{18}O$ may aid the interpretation of the underlying physiological processes (Scheidegger et al. 2000). The explanatory power of isotope analyses is still limited due to several factors of uncertainty (Roden and Siegwolf 2012); The oxygen isotopic composition itself is on the one hand influenced by the signature of the source water and also by leaf water enrichment due to transpiration, related to atmospheric condition and stomatal conductance (McCarroll and Loader 2004; Gessler et al. 2014). Additionally, an exchange between oxygen of the assimilates and water during transport in the phloem or cellulose synthesis may occur (Gessler et al. 2009, 2014), potentially uncoupling the signal in the leaf and the wood (Offermann et al. 2011) and thus also limiting the interpretation in the terms

of physiological response to atmospheric conditions. When interpreting the isotopic composition of carbon and oxygen in the stem wood, it also has to be considered that if stored carbohydrate reserves are remobilised, their isotopic signature is mixed with that of recently assimilated carbon, potentially also changing the relationship between oxygen and carbon (Roden and Siegwolf 2012; Gessler et al. 2014). Despite those potential constraints, various studies have found annual $\delta^{13}C$ and/or $\delta^{18}O$ of stem wood to be well correlated with various climatic variables such as temperature, precipitation and/or VPD (Hartl-Meier et al. 2015; Vitali et al. 2021). Additionally, the intrinsic water-use efficiency (WUE_i) as calculated from $\delta^{13}C$ in tree rings is an indicator of the ratio of net photosynthetic rate to stomatal conductance and can give an insight into general growth and drought tolerance strategies of trees (Gessler et al. 2018).

In this study, we investigated (1) how stem diameter growth and stable isotopic composition of carbon and oxygen in the wood respond to climatic variation in urban trees to find out (2) which tree species are particularly vulnerable to drought as indicated by low resistance/resilience of stem diameter growth, increased $\delta^{13}C$ and $\delta^{18}O$ as well as changing WUE_i. Additionally, we aimed to analyse (3) if the exposition to NO_x emissions from traffic is reflected in the stable isotopic composition of nitrogen in the stem wood and, finally (4), if there is an interplay between the intensity of traffic emissions and the reaction of stem growth to drought.

Material

Study area

The study was conducted in the neighbouring cities of Karlsruhe and Rheinstetten, which are located in the Northwest of the state of Baden-Württemberg in Southwest Germany and cover a total area of 206 km^2. Karlsruhe has a population of ~313,000 and Rheinstetten of ~21,000 inhabitants. About one-third of their area is classified as forest, while about 30 % of the area is urban fabric composed of residential areas, commercial districts, roads and other sealed as well as green urban areas. The remaining area comprises arable land, water and port areas, railways and other types of land use (Copernicus Land Monitoring Service 2021). This study area was chosen as it allows to analyse trees on a gradient ranging from the inner area of a large city and its outskirts to a small town.

Data on climate and traffic pollution

Data on monthly temperature means and precipitation sums were obtained from the German Weather Service DWD (DWD

Climate Data Center (CDC) 2020a, 2020b). These gridded raster data have a resolution of 1×1 km, interpolated based on weather station data. It is important to note that processes characteristic for urban climate such as urban heat island effects are not represented by this data.

Two different types of geospatial data were used to characterise the pollution intensity within the study area. Data on the background NO_2 concentration (for the year 2010) with a spatial resolution of 0.5×0.5 km as provided by the Environmental Agency of Baden-Wuerttemberg (LUBW 2014) were used to split the study area into three areas of general pollution intensity (i.e. high intensity in the inner city of Karlsruhe [$> 30\ \mu g\ m^{-3}$], medium intensity in the outskirts of Karlsruhe [24–$30\ \mu g\ m^{-3}$] and low intensity in the city of Rheinstetten [$< 24\ \mu g\ m^{-3}$]). This dataset is based on the interpolation of measurements in combination with a chemical transport model (LUBW 2014). To characterise the emission load due to traffic for each of the selected sample trees we referred to the emission inventory for the year 2014 (LUBW 2017), which provides data on the NO_x emission by traffic with a spatial resolution of 0.5×0.5 km based on a compilation of data from various sources such as traffic counts in combination with emission factors.

Sample trees

Five deciduous broadleaved tree species, which are among the most abundant urban tree species in the study area, were selected: *Acer platanoides* (15 %), *Quercus robur* (8 %), *Carpinus betulus* (7 %), *Tilia cordata* (6 %) and *Platanus×hispanica* (4 %). Within each of the three defined areas of high, medium and low intensity of NO_2 pollution (s. above), at least ten trees per species were selected. Further, half of those trees were chosen to be located directly at streets and the other half in parks or other sites without direct influence from (high traffic) roads. This selection was carried out based on the tree cadastres provided by the cities of Karlsruhe and Rheinstetten as well as the road types provided by OpenStreetMap (OpenStreetMap contributors 2021). The sample trees were further selected to have a diameter at breast height ($d_{1.3}$) of at least 40 cm in order to guarantee tree ring series with a length of > 30 years. In few cases (< 15), trees with smaller $d_{1.3}$ had to be chosen so as to fulfil the other criteria. The elevation of the sampled trees varied only slightly (103–117 m a. s. l.), so that we conclude that this factor is likely not influential for our analysis. In total, 166 sample trees were considered for the analysis. Spatial data processing and tree selection were carried out in QGIS 3.2 (QGIS.org 2021).

Methods

Sampling and data preparation

Field work was carried out between September 2019 and April 2020. For each sample tree, the diameter at breast height (1.3 m), tree height, height of the crown base and crown projection area were measured. A mixed soil sample was collected at a soil depth of 0–40 cm in vicinity of the stem base. In few cases it was not possible to collect a soil sample or only up to a reduced depth due to (artificial) soil compaction/sealing. The soil samples were analysed for the following parameters: Soil texture (according to VDLUFA 1991), pH (CaCl$_2$, according to VDLUFA 1991), cation exchange capacity and sum of base cations (according to DIN EN ISO 11260:2011-09), total organic carbon (according to DIN EN 15936:2012-11). As an indicator for salinity due to de-icing salt, soil electrical conductivity (at 25 °C) was measured (according to DIN ISO 11265:1997-06). As a further indicator for the intensity of traffic, the contents of lead (Pb) and cadmium (Cd) were analysed (according to DIN EN 13657:2003-01). Base saturation (BS) was calculated as BS (%) = (sum of base cations)/(cation exchange capacity) × 100.

For each sample tree, two tree cores were extracted, with one core being extracted perpendicular and one core parallel to the street. The extracted cores were air dried, mounted in plastic holders and the surface removed with a diamond fly cutter to enhance the visibility of the tree ring boundaries (Spiecker et al. 2000). The core surfaces were scanned with a flatbed scanner and the tree ring boundaries defined in WinDendro (Regent Instruments Inc., Canada) or—in the case of *C. betulus*—measured with a measurement table (VIAS, Austria) and a stereo microscope using the software Past4 (SCIEM, Austria). When necessary, the surface was further prepared with sharp razor blades. If the pith was not present on the core, the number of missing rings was estimated from the curvature of the innermost rings to estimate tree age. In few cases where rings did not show any curvature, the number of missing rings was reconstructed based on the difference between the length of the core and the tree radius (assumed to equal half of the measured $d_{1.3}$) as well as the average width of the 30 innermost rings for *P. × hispanica* and the 10 innermost rings for the remaining species.

Tree ring chronologies

For each tree, the annual ring widths of the two cores were averaged. The resulting tree ring series were detrended by fitting a cubic smoothing spline with a 50 % frequency cut-off at a length of 15 years and the annual tree ring width indices (RWI) calculated by dividing the measured tree ring width (TRW) by the expected value of the fitted spline (Fritts 1976). If present, autocorrelation in the series was removed by fitting an ARIMA model, where the best model was chosen based on the Bayesian information criterion (BIC). For each species, the Expressed Population Signal (EPS) and mean Gleichläufigkeit (GLK) were calculated. Chronologies for each species were built by calculating the annual Tukey's biweight robust mean for the period 1982–2018, which is covered by at least two thirds of all trees within each species. These steps were carried out in *R* with the packages *dplR* and *forecast* (R Core Team 2020; Bunn et al. 2021; Hyndman et al. 2021).

Analysis of carbon, oxygen and nitrogen stable isotopes

For the analysis of the stable isotopic composition of the carbon and oxygen content in the tree rings, six trees per species were selected by stratified random sampling based on the pollution intensity and the distance to the street to cover all six combinations (three pollution intensity levels × two locations [street or park]). Due to technical difficulties *C. betulus* could not be considered for isotope analysis. For each of the selected trees one core was mechanically separated into annual segments for the time period 2000–2018 (for *Q. robur* only latewood was used). For the analysis of the isotopic composition of the nitrogen content in the wood one segment covering the time period 2012–2018 was cut from 30 randomly selected trees per species.

The samples were prepared by applying a Soxhlet extraction with first methylene dichloride and then methanol and then sand-dried overnight at 60 °C. Samples were milled with a ball mill (or broken up with a scalpel if the quantity was low) and weighed into tin capsules. For the measurement of $\delta^{18}O$, samples were equilibrated in laboratory water overnight in a desiccator with lithium chloride (air humidity of 11.3 %) and then vacuum dried for > 2 h in the desiccator. For the measurement of $\delta^{15}N$, four measurements were carried out for each sample, and for $\delta^{13}C$ and $\delta^{18}O$, two measurements were carried out for each sample in an isotope mass spectrometer (Nu Instruments, UK). Each test run was preceded by the measurement of eight laboratory standards. During the test run of $\delta^{13}C$, two laboratory standards were measured every 12 samples, while 6 laboratory standards were measured at regular intervals for $\delta^{18}O$. Due to the low nitrogen concentrations, each test run included between 20 and 25% standards. Isotope ratios are expressed as $\delta^{13}C$ relative to VPDB, $\delta^{18}O$ relative to VSMOW and $\delta^{15}N$ relative to air. Due to the increased burning of fossil fuels since the industrial revolution there has been a decline in $\delta^{13}CO_2$, which has to be accounted for when analysing

the isotopic composition of carbon in tree rings (McCarroll and Loader 2004; Belmecheri and Lavergne 2020). Therefore, the $\delta^{13}C$ values measured in the tree rings were corrected based on the pre-industrial value of $\delta^{13}CO_2$, assumed to be $-6.4‰$ (McCarroll and Loader 2004; Belmecheri and Lavergne 2020), and monthly measurements of the isotopic composition of $\delta^{13}CO_2$ at the Mauna Loa Observatory, Hawaii (Keeling et al. 2005). Based on the annual mean value of these data, an annual offset was calculated with which the measured $\delta^{13}C$ values were corrected. All further analyses are based on these corrected values. As the visual inspection of the resulting series suggested the existence of linear trends in few series, the individual series of $\delta^{13}C$ and $\delta^{18}O$ were tested for such linear trends, which occurred in six series of $\delta^{13}C$ and five series in $\delta^{18}O$. Those series were detrended linearly based on the residuals of the linear regression and the mean value of the time series in order to keep the original scale. The (detrended) series were then tested for autocorrelation by fitting an ARIMA model and autocorrelation was removed if present (s. above).

The annual intrinsic water use efficiency (WUE_i) of each tree was calculated from the annual $\delta^{13}C$ values for the period 2000–2018 according to Farquhar et al. (1982; Eq. 1), where ca is the atmospheric CO_2 concentration (ppm), $\delta^{13}C_{atm}$ the carbon isotopic composition of atmospheric CO_2 (‰), $\delta^{13}C_r$ the carbon isotopic composition of the individual radial growth tree rings (‰), a the isotope fractionation during CO_2 diffusion through the stomata (4.4 ‰), b the isotope fractionation during carboxylation (27 ‰) and 1.6 the ratio of the molar diffusivity of H_2O to CO_2 in air.

$$WUE_i = \frac{A}{g_s} = \frac{ca}{1.6} \times \left(\frac{b - \delta^{13}C_{atm} + \delta^{13}C_r}{b - a} \right) \quad (1)$$

The mean annual atmospheric CO_2 concentration and isotopic composition of $\delta^{13}CO_2$ were obtained from monthly measurements of the Mauna Loa Observatory, Hawaii (Keeling et al. 2005; Keeling and Keeling 2017).

Significant differences in mean $\delta^{13}C$, $\delta^{18}O$ and WUE_i (for the whole time period) between species were assessed based on pairwise comparisons of the estimated marginal means of a linear mixed model of the form in Eq. (2), where y_i is the response variable ($\delta^{13}C$, $\delta^{18}O$ or WUE_i), X_i and β are the design matrix and parameter vector for the fixed effect (species), Z_i and b_i are those for the random effect (tree), and ε_i is the residual error, which is assumed to be normally distributed.

$$y_i = X_i\beta + Z_i b_i + \varepsilon_i \quad (2)$$

For species differences in wood $\delta^{15}N$ as well as the influence of the tree position regarding the distance to the street and the exposition to traffic emissions, a linear model was fit with $\delta^{15}N$ as the response variable, and the species, the distance to the nearest street (log-transformed) and the intensity of NO_x emissions as fixed effects. All analyses were carried out in *R* with the packages *lme4* and *emmeans* (Bates et al. 2015; R Core Team 2020; Lenth 2021). The relative contribution of each predictor to the explained variance was assessed based on its average squared semi-partial correlations calculated over all possible permutations of the predictors, using the package *relaimpo* in *R* with the metric *lmg* (Grömping 2006, 2015).

Correlations of RWI, $\delta^{13}C$ and $\delta^{18}O$ series with climate

Relationships between the chronologies of ring width indices (RWI), $\delta^{13}C$ and $\delta^{18}O$ and monthly climate parameters were assessed by calculating Pearson's correlation coefficients for monthly values of precipitation and temperature in the vegetation period (March–August) as well as the mean temperature and precipitation sum of the preceding summer (June–August) and autumn/winter (September–February). The analysis was conducted in *R* with the package *treeclim* (Zang and Biondi 2015; R Core Team 2020).

Drought response and its influences

Years with exceptional drought periods were identified based on the standardised precipitation-evapotranspiration index (SPEI). A threshold value of -1.35 was identified by calculating the 10th percentile of the SPEI values of August (with a scale of 6 months as an indicator of water availability during the vegetation period) for the time period 1900–2018. Years between 2000 and 2015 with SPEI-6 values in August of -1.35 or lower were considered for the further analysis. PET (after Thornthwaite) and SPEI values were calculated in *R* with the package *spei* (Beguería and Vicente-Serrano 2017; R Core Team 2020).

The growth reaction to drought in the identified years was analysed based on the indices resistance and resilience (Lloret et al. 2011), relating the ring width in the year of the drought to the mean pre-drought ring width (termed *resistance*, *Rt*), and the mean post-drought to the mean pre-drought ring width (termed *resilience*, *Rs*). The analysis was conducted in *R* with the package *pointRes* (van der Maaten-Theunissen et al. 2015; R Core Team 2020), employing the raw ring width series (averaged per tree) and a reference period for mean pre- and post-drought growth levels of 3 years each.

To test the indices for significant deviations from 1 (i.e. a significant difference from the pre-drought growth level) as well as for significant differences between species and drought periods (i.e. years), a linear mixed model of the form in Eq. (3) was fit, where y_i is the response variable (resistance or resilience), X_i and β are the design matrix

and parameter vector for the fixed effect (species, year and their interaction), Z_i and b_i are those for the random effect (tree), and ε_i is the residual error. The response variables were log-transformed to ensure normal distribution of residuals.

$$\log y_i = X_i\beta + Z_ib_i + \varepsilon_i \qquad (3)$$

The estimated marginal means for each species and year were first tested against the null hypothesis of no significant difference from the pre-drought growth level. Then, pairwise comparisons were carried out (both between and within species/years) based on Tukey-adjusted p values. The analyses were carried out in *R* with the packages *lme4* and *emmeans* (Bates et al. 2015; R Core Team 2020; Lenth 2021).

To explain the intra-specific variation of the calculated indices resistance and resilience, a linear mixed model of the form in Eq. (3) was built with predictors that characterise the individual trees (mean basal area increment in the three years preceding the drought [mean BAI_{pre}], basal area at 1.3 m stem height [BA] and tree age in the drought year) as well as soil parameters (soil texture, pH value, base saturation [BS], soil electrical conductivity [SEC], total organic carbon content [TOC], Pb and Cd content) and site (distance to the nearest street, NO_x emissions from traffic) as fixed effects. The predictor year (2003, 2011, 2015) was included as a categorical fixed effect to account for systematic differences in drought response caused by differing drought conditions (timing, duration and intensity). The predictors were standardised (i.e. centred and scaled) for ease of interpretation of the coefficients. For each of the species a separate model was fit with tree as a random effect. The analysis was carried out in *R* using the packages *lme4*, *lmerTest* and *effectsize* (Bates et al. 2015; Kuznetsova et al. 2017; Ben-Shachar et al. 2020; R Core Team 2020).

To facilitate the interpretation of significant deviations from the mean, the time series of $\delta^{13}C$ and $\delta^{18}O$ were standardised to a mean of 0 and a standard deviation of 1 and annual values were averaged for each species to obtain species-specific chronologies of $\delta^{13}C$ and $\delta^{18}O$. We tested for each species (n_{trees} per species = 6) if the annual value of $\delta^{13}C$ in the year of the drought or the subsequent year is significantly higher than 0 (i.e. the mean) by applying a one-sample t test. For $\delta^{18}O$ we tested if the standardised value is significantly different from 0 with a two-sided one-sample *t* test. Additionally, mean values for $\delta^{13}C$ and $\delta^{18}O$ (2000–2018) and *Rt* (2003, 2011 and 2015) were calculated and the Pearson's correlation was calculated between those variables across species (n_{trees} = 24). All calculations were carried out in *R* (R Core Team 2020).

Results

Sample trees and site conditions

The mean $d_{1.3}$ ranged from 45 cm for *C. betulus* to 64 cm for *P.* × *hispanica*. The mean tree height was also greatest in *P.* × *hispanica* (21 m), and smallest in *C. betulus* and *A. platanoides* (17 m). Accordingly, *P.* × *hispanica* trees had the greatest average crown length and crown projection area, while *T. cordata* trees had the smallest mean crown projection area. Here, it has to be considered that especially roadside trees are regularly pruned, so that tree height, crown height and crown projection area are subject to strong artificial influence and only represent a "snapshot" of the appearance at the time of measurement. An overview of the number of trees per species, the mean diameter at breast height, tree height, crown length and crown projection area is given in Table 1. Across all sampled tree species, NO_x emissions from traffic as estimated for the year 2014 ranged between

Table 1 Overview of diameter at breast height, tree height, crown length and crown projection area of the sample trees (mean ± standard deviation) at the time of sampling, n = 166

Species	A. platanoides	C. betulus	P. × hispanica	Q. robur	T. cordata
n_{trees}	34	30	38	33	31
Tree age [years]	68 ± 27	71 ± 39	58 ± 18	82 ± 55	70 ± 31
Diameter at 1.3 m [cm]	50.7 ± 7.5	44.6 ± 6.5	64.1 ± 17.3	62.7 ± 19.0	47.6 ± 5.6
Height [m]	16.8 ± 3.7	16.6 ± 3.4	21.0 ± 3.5	19.6 ± 4.7	17.8 ± 3.0
Crown length [m]	13.2 ± 2.5	13.9 ± 2.8	17.5 ± 3.8	15.2 ± 3.7	13.6 ± 2.9
Crown projection area [m²]	95.9 ± 37.3	85.37 ± 33	150 ± 67.5	120 ± 45.7	70.9 ± 24.1
EPS_{RWI}	0.93	0.92	0.96	0.93	0.88
GLK_{RWI} [%]	58	60	63	60	56
n_{trees}	6	–	6	6	6
$\delta^{13}C$ [‰]	− 23.3 ± 1.15	NA	− 24.6 ± 0.78	− 24.5 ± 1.25	− 24.1 ± 0.74
$\delta^{18}O$ [‰]	27.2 ± 0.88	NA	23.8 ± 0.67	25.5 ± 0.77	26.8 ± 0.84
WUE_i [μmol CO_2 mol⁻¹ H_2O]	108 ± 7.43	NA	94.6 ± 4.72	95.0 ± 5.04	99.5 ± 5.55

Chronology statistics (EPS_{RWI} and GLK_{RWI}) are given for the period 1982–2018, and values for $\delta^{13}C$, $\delta^{18}O$ and WUE_i (mean ± standard deviation of six trees per species) for the period 2000–2018

0 and 15.872 kg. The distance to the nearest (main) road ranged from 2.2 to 593.2 m, with 75 % of the trees being located within a distance of 73 m. Concerning the soil, 42 % of the soil samples were classified as weakly loamy sand and 27 % as strongly loamy sand. Further 22 % represented sandy loam and 3 % silty loam. Soil texture was sand for 5 % of the samples and 1 % ($\triangleq$ one sample) could not be classified. The mean pH value was 6.38 ± 0.91 [standard deviation], the total organic carbon content 2.83 ± 2.49 % and the base saturation 82 ± 20 %. The mean soil electrical conductivity (at 25 °C) was 103.5 ± 60.3 μS cm^{-1}. The mean lead (Pb) content was 86.33 ± 255.25 mg kg dry soil^{-1} and the mean cadmium (Cd) content 0.49 ± 0.46 mg kg dry soil^{-1} (data not shown).

Species-specific tree ring chronologies and mean δ¹³C, δ¹⁸O and WUE_i

The common variance of the individual series of tree ring indices was highest in *P. × hispanica*, followed by *Q. robur*, *A. platanoides*, *C. betulus* and *T. cordata*, as shown by the expressed population signal (EPS) and mean Gleichläufigkeit (GLK) in Table 1. The chronologies of the five species are shown in Fig. 1.

For the time period 2000–2018, the mean value for δ¹³C ranged from -23.3 ‰ in *A. platanoides* to -24.6 ‰ in *P. × hispanica*, with no significant differences between species. The mean value for δ¹⁸O was lowest in *P. × hispanica*, and highest in *A. platanoides*. Here, pairwise comparisons revealed significant differences between all species but between *A. platanoides* and *T. cordata*. The mean intrinsic

water-use efficiency (WUE_i) was higher in *A. platanoides* than in the other three species but differences between species were not significant at $p < 0.05$. All values are given in Table 1. The time series of annual mean WUE_i of each species are shown in Fig. 2.

Relationships of tree ring indices, carbon and oxygen isotopes with climate

In all species except *P. × hispanica* precipitation in May was positively correlated with ring width (ranging between $r = 0.32$ in *C. betulus* and $r = 0.57$ in *T. cordata* (Table 2). In addition, there existed a positive relationship between precipitation in March and ring width in *C. betulus* ($r = 0.29$), *P. × hispanica* ($r = 0.28$) and *Q. robur* ($r = 0.36$), the latter also being the only tree species to exhibit a significant correlation between TRW and precipitation in June ($r = 0.36$). Precipitation in July was positively correlated with tree ring index in *T. cordata* ($r = 0.24$). *P. × hispanica* was the only species showing a significant correlation between the precipitation of the previous summer and TRW ($r = 0.37$). Concerning temperature, there was a negative correlation between March temperature and tree ring index in *Q. robur* and *T. cordata* ($r = -0.47$ and -0.33, respectively). In contrast, tree ring growth in *P. × hispanica* was positively related with April temperature ($r = 0.38$). In *A. platanoides* and *C. betulus* tree ring growth was negatively affected by high temperatures in the previous summer ($r = -0.29$ and -0.44, respectively). Only in *A. platanoides* and *T. cordata* significant correlations between δ¹³C and climate variables were found (note that no isotope analysis was

Fig. 1 Chronologies of ring width indices (RWI) for the time period 2000–2018. The three years with exceptional droughts (2003, 2011 and 2015) are highlighted by light grey vertical bars
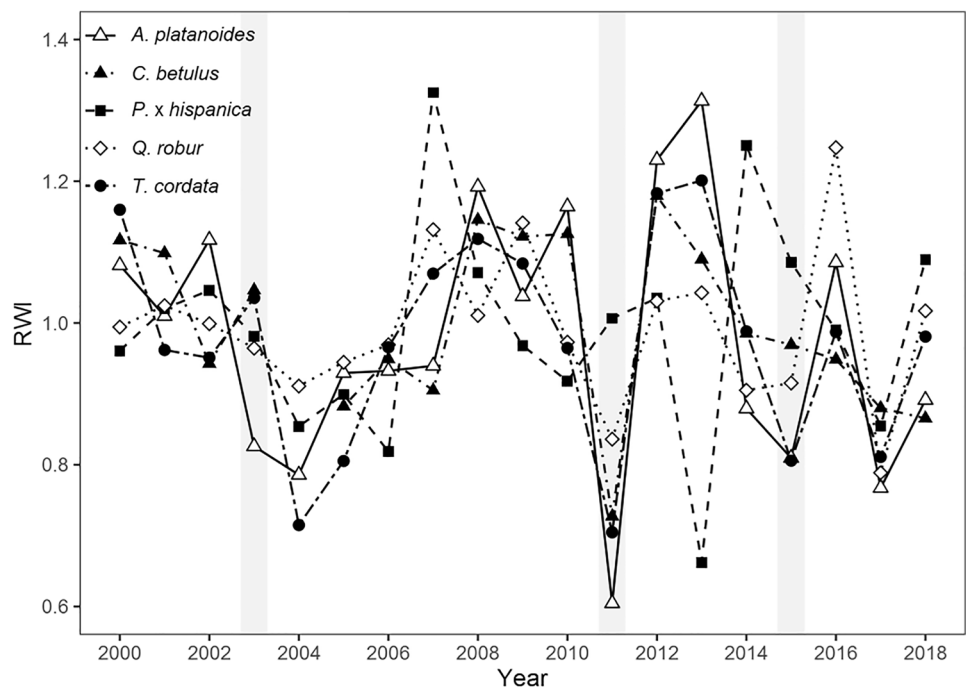
Fig. 2 Annual intrinsic water-use efficiency (WUE$_i$) for the time period 2000–2018. The three years with exceptional droughts (2003, 2011 and 2015) are highlighted by light grey vertical bars
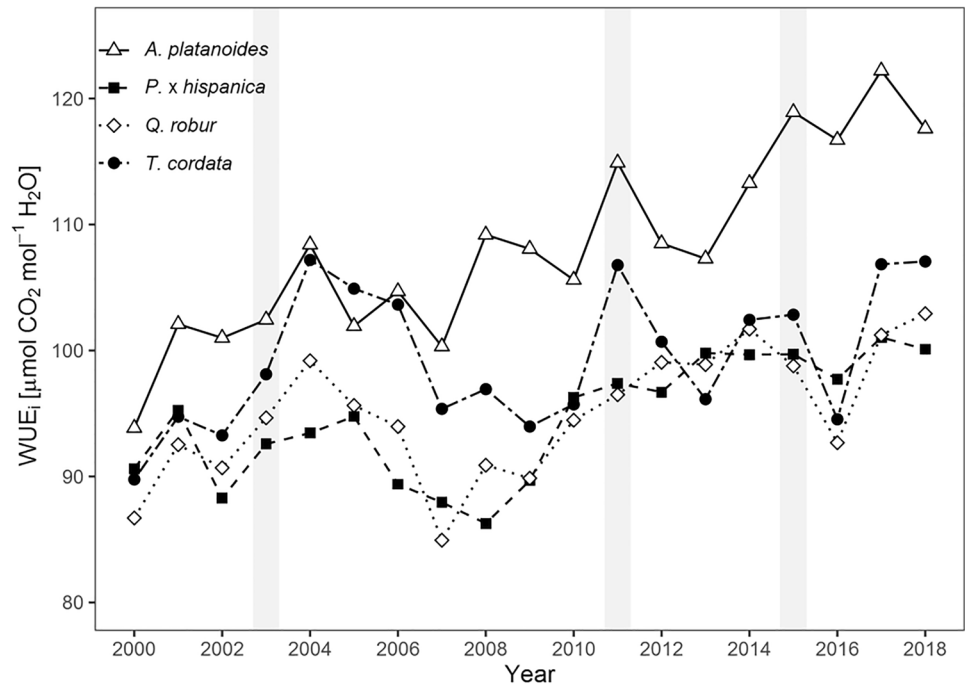

Table 2 Pearson's correlation coefficients between climate variables and ring width index (RWI; 1982–2018), $\delta^{13}C$ and $\delta^{18}O$ (2000–2018)

Species	Precipitation					Temperature					
	Mar	May	Jun	Jul	Sum prev JJA	Mar	Apr	May	Jul	Aug	Mean prev JJA
A. platanoides											
RWI		0.43									− 0.29
$\delta^{13}C$		− 0.68								0.36	
$\delta^{18}O$		− 0.43							0.24		
C. betulus											
RWI	0.29	0.32									− 0.44
P. × hispanica											
RWI	0.28			0.37			0.38				
$\delta^{13}C$											
$\delta^{18}O$		− 0.63		0.29					0.42		
Q. robur											
RWI	0.36	0.53	0.36			− 0.47					
$\delta^{13}C$											
$\delta^{18}O$		− 0.53									
T. cordata											
RWI		0.57	0.24			− 0.33					
$\delta^{13}C$		− 0.52									
$\delta^{18}O$		− 0.3									

Only climate variables with at least one significant correlation are shown

carried out for *C. betulus*)—in both species precipitation in May was negatively correlated with $\delta^{13}C$ values ($r = - 0.68$ and − 0.52, respectively). In *A. platanoides*, $\delta^{13}C$ was also positively related to August temperature ($r = 0.36$). In all four species precipitation in May was negatively correlated with $\delta^{18}O$ (between $r = - 0.3$ in *T. cordata* and $r = - 0.63$ in

P. × hispanica). *P. × hispanica* was the only species with a significant relationship between $\delta^{18}O$ and the previous summer's precipitation ($r = 0.29$). In this species, $\delta^{18}O$ was also positively related to temperature in May ($r = 0.42$), while such a positive correlation was found for July temperature

in *A. platanoides* ($r = 0.24$). An overview of all significant correlations is provided in Table 2.

Factors influencing δ¹⁵N

The linear mixed model explained 54 % of the variance of $\delta^{15}N$ ($p < 0.001$). The predictor species accounted for 75 % of this explained variance with $\delta^{15}N$ levels being significantly different between all species but between *Q. robur* and *T. cordata*. Estimated marginal means (± standard error) were highest in *P. × hispanica* (4.96 ± 0.32 ‰), followed by *A. platanoides* (2.56 ± 0.32 ‰), *Q. robur* (1.40 ± 0.31 ‰) and *T. cordata* (1.19 ± 0.32 ‰). Distance to the nearest street had a negative effect on $\delta^{15}N$ and the intensity of NO_x emissions from traffic a positive effect (Table 3).

Years with exceptional drought periods

For the period 2000–2015, three years were identified as years with severe drought periods, i.e. had a mean SPEI-6 (for August) of − 1.35 or lower. These years were 2003 (− 2.32), 2011 (− 1.46) and 2015 (− 2.10). In 2003, SPEI-3 values were ≤ − 1.35 from April to September with the drought being most severe in August (− 2.14). In 2011, the drought period lasted from March to June with the highest severity in May (− 2.41). In 2015, values were first below − 1.35 in July and the drought lasted throughout the growing season, with the lowest SPEI-3 value occurring in August (− 1.96) (Fig. 3).

Table 3 Coefficients and proportions of explained variance for the predictors of the linear model ($n = 119$) with $\delta^{15}N$ as response variable and *A. platanoides* as the reference level for the predictor species

	Coefficient ± se	*p* value	Proportion of explained variance (%)
Intercept	4.062 ± 0.465	< 0.001	
Species			
P. × hispanica	2.394 ± 0.428	< 0.001	75
Q. robur	− 1.376 ± 0.426	0.002	
T. cordata	− 1.161 ± 0.432	0.008	
log(distance to nearest road)	− 0.501 ± 0.115	< 0.001	16
NO_x emissions from traffic	0.196 ± 0.051	< 0.001	9

Fig. 3 Monthly temperature means and precipitation sums in 2003, 2011, and 2015 (with 30-year average of the period 1981–2000 shown as solid line) as well as monthly SPEI-3 values
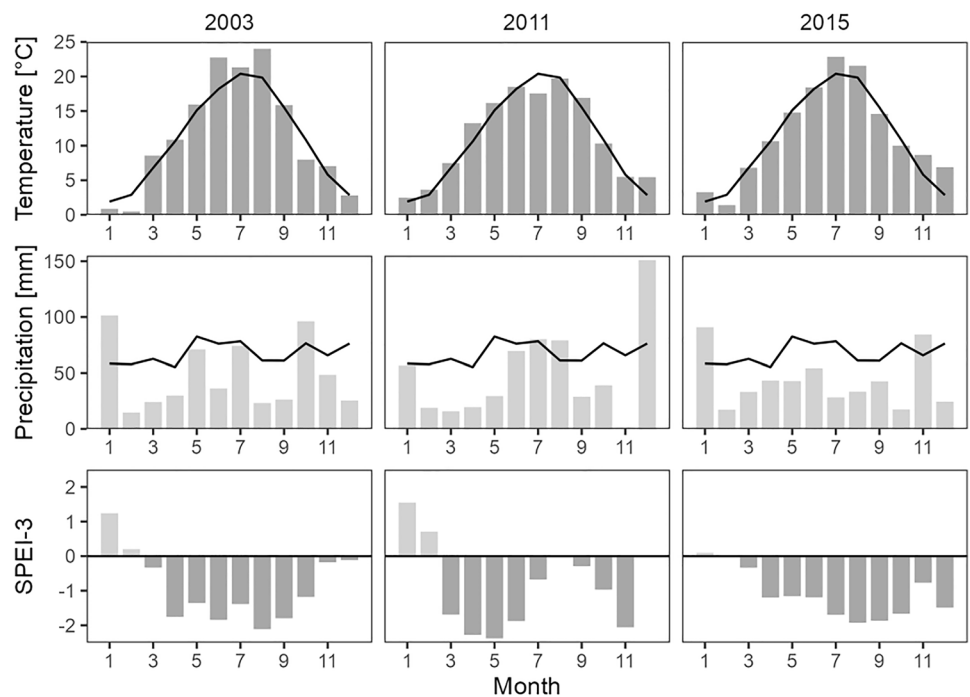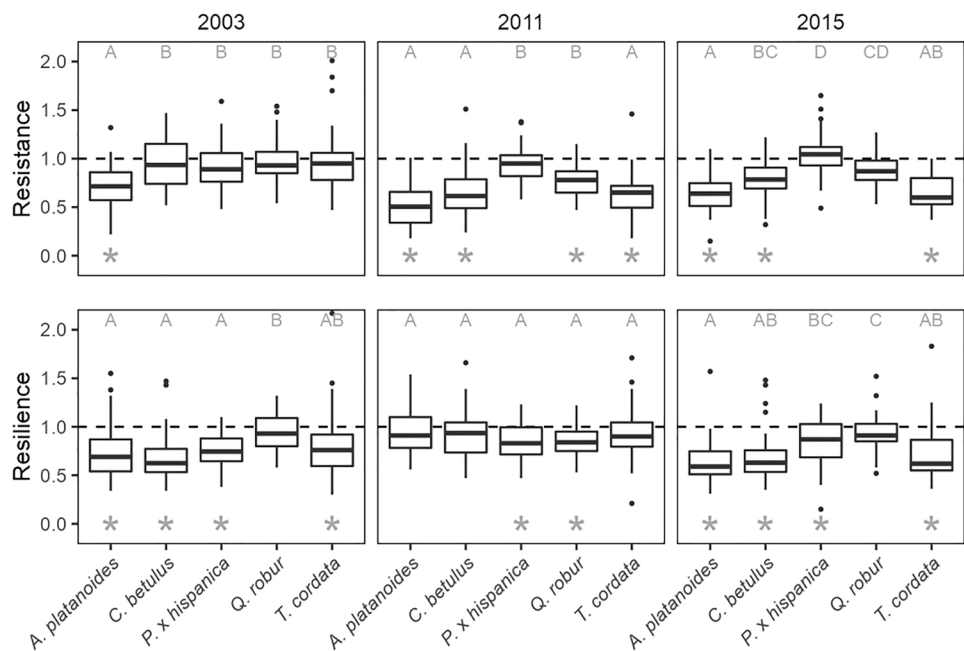
Resistance and resilience to drought and their influencing factors

Across the three years, resistance in *A. platanoides* was significantly lower than in the other four species (0.59 ± 0.02), and resistance in *T. cordata* and *C. betulus* significantly lower than in *Q. robur* and *P.* × *hispanica* (0.71 ± 0.03 and 0.74 ± 0.03 compared to 0.86 ± 0.03 and 0.94 ± 0.03, respectively). Across all species, resistance differed significantly between the three years considered. It was lowest in 2011 (0.66 ± 0.02), followed by 2015 (0.77 ± 0.02) and 2003 (0.86 ± 0.02). In 2003, *A. platanoides* showed a significant growth reduction, while the estimated resistance did not differ significantly from 1 for the other species (Fig. 4). In 2011, all species but *P.* × *hispanica* showed a significantly reduced TRW. In 2015, growth was not significantly reduced in *P.* × *hispanica* and *Q. robur* while *A. platanoides* and *T. cordata* showed the lowest resistance.

Across all years, the estimated marginal mean of resilience to drought was significantly higher in *Q. robur* (0.9 ± 0.03) than in all other species (*C. betulus* $= 0.72 \pm 0.02$, *A. platanoides* $= 0.73 \pm 0.02$, *T. cordata* $= 0.78 \pm 0.03$, *P.* × *hispanica* $= 0.78 \pm 0.02$). Across all species, resilience was significantly highest after 2011 (0.87 ± 0.02) and similar after 2003 and 2015 (0.75 ± 0.02 and 0.72 ± 0.02, respectively). After 2003, the estimated mean resilience was significantly below 1 for all species but *Q. robur* (Fig. 4). After 2011, however, resilience was significantly below 1 for *P.* × *hispanica* as well as *Q. robur* while the mean post-drought growth levels were similar to the pre-drought levels in *C. betulus*, *T. cordata* and *A. platanoides*. As in 2003, all species except *Q. robur* showed an estimated mean resilience below 1 after 2015.

Modelling potential effects of site conditions as well as tree-individual characteristics to explain intra-specific variability in resistance and resilience revealed that for none of the tree species there was a significant effect of the tree's distance to the nearest street nor of the general level of NO_x emissions from traffic (Table 4). Further, only *A. platanoides*, *P.* × *hispanica* and *T. cordata* showed resistance or resilience to be affected by soil conditions: the resistance of *T. cordata* was positively affected by the total organic carbon content and in *A. platanoides,* resistance was higher in trees growing in weakly as well as in highly loamy sand (compared to reference level sand). Further, in *T. cordata*, tree age (in the year of the drought) had a negative effect on resistance, and in *A. platanoides*, *C. betulus* and *T. cordata* resilience was negatively related to the pre-drought growth level (BAI_{pre}). There also was a strong positive effect of resistance on resilience, i.e. within each species, trees with a strong growth inhibition in the year of the drought also showed relatively low post-drought growth compared to the pre-drought levels.

Carbon and oxygen stable isotope signals in and after years with drought and their relationship with drought resistance

None of the four species showed significantly increased values of $\delta^{13}C$ in 2003. However, for *Q. robur* and *T. cordata* $\delta^{13}C$ values were significantly higher than average in the following year (2004). *T. cordata* as well as *A. platanoides* showed significantly increased $\delta^{13}C$ values in 2011. $\delta^{13}C$ was not significantly increased in any of the species in or after 2015 (Fig. 5).

Fig. 4 Box plots of resistance and resilience of the five species in/after the years 2003, 2011, and 2015. Asterisks mark significant differences of estimated marginal means from 1, and letters indicate significant differences between species (based on pairwise comparisons) within years. Three outliers (resilience for *A. platanoides* [2.24] and *T. cordata* [2.75] in 2003 and for *T. cordata* [2.17] in 2011 are not shown for better visibility)

Table 4 Estimated standardised coefficients for the linear mixed models with the response variables resistance and resilience

	Resistance					Resilience				
	A. pla	*C. bet*	*P. ×his*	*Q. rob*	*T. cor*	*A. pla*	*C. bet*	*P. ×his*	*Q. rob*	*T. cor*
n_{obs} (n_{trees})	99 (33)	84 (28)	105 (35)	93 (31)	81 (27)	99 (33)	82 (28)	105 (35)	93 (31)	81 (27)
sd ID	0.15	0.20	0.16	0.18	0.00	0.10	0.1	0.00	0.16	0.07
sd Residuals	0.28	0.30	0.29	0.27	0.32	0.29	0.28	0.25	0.26	0.28
Soil texture										
Sand	–	RL	RL	RL	–	–	RL	RL	RL	–
Sandy loam	RL	0.11	0.17	0.24	RL	RL	0.03	0.24	0.06	RL
Silty loam	0.45	–	− 0.03	0.53	− 0.09	0.02	–	0.34	0.19	0.59
Weakly loamy sand	**0.31**	0.19	0.26	0.30	0.20	− 0.10	0.03	0.13	− 0.10	− 0.06
Strongly loamy sand	**0.42**	0.12	0.19	0.54	0.00	− 0.01	0.07	0.12	− 0.02	− 0.02
TOC	− 0.06	0.05	− 0.07	− 0.03	**0.22**	− 0.07	0.05	0.04	0.02	− 0.03
Mean BAI$_{pre}$	− 0.04	− 0.04	− 0.06	− 0.09	− 0.02	**− 0.09**	**− 0.19**	0.00	− 0.12	**− 0.20**
Age	− 0.02	0.03	− 0.08	− 0.12	**− 0.15**	− 0.11	− 0.05	0.04	0.02	− 0.12
log(Rt)	–	–	–	–	–	**0.36**	**0.29**	**0.42**	**0.52**	**0.36**
R^2_m	0.3	0.2	0.24	0.26	0.41	0.41	0.50	0.29	0.35	0.41
R^2_c	0.44	0.45	0.42	0.49	0.41	0.47	0.56	0.29	0.53	0.45

For each species, the number of trees (n_{trees}) and observations (n_{obs}), the standard deviation of ID and the residuals are shown. For each predictor, the standardised coefficient is displayed. Significant effects ($p < 0.05$) are printed in bold. Coefficients for the levels of the categorical predictor year ($n = 3$; 2003, 2011 and 2015) are not shown. For each model, the marginal and conditional R^2 values are given. Note that parameters mean BAI$_{pre}$, BA and age vary by tree and year, while soil and site parameters vary by tree only. Coefficients for pH value, BS (base saturation), SEC (soil electrical conductivity), Pb (lead content of the soil), Cd (cadmium content of the soil), NO$_x$ emissions, distance to the nearest street and BA (basal area in the year of the drought) are not shown as their effects were not significant in any of the models. *RL* marks the respective reference level for the categorical predictor soil texture

TOC total organic carbon, *mean BAI$_{pre}$* mean basal area increment in the 3 years preceding the year of the drought, *Rt* resistance.

Fig. 5 Mean (± standard deviation as light and dark grey ribbons) of standardised series of δ^{13}C (solid lines) and δ^{18}O (dashed lines). For δ^{13}C, significantly elevated values in the year of the drought (solid vertical lines) or subsequent year (dotted vertical line) are marked by the cross symbol, and for δ^{18}O values significantly different from 0 are marked by the asterisk symbol
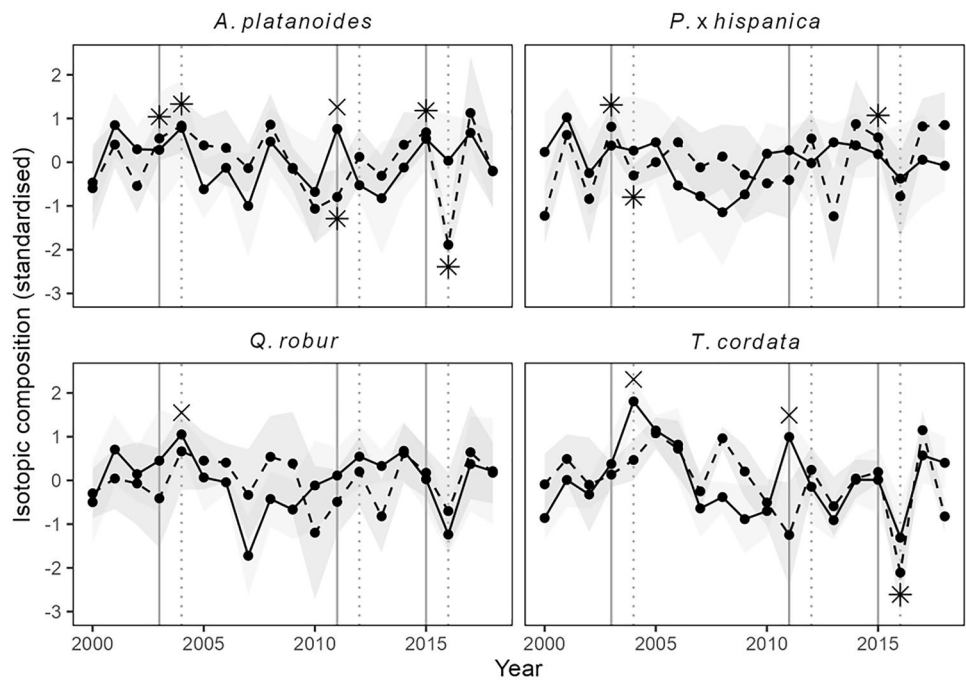
Concerning δ^{18}O, values were significantly higher than average in 2003 and 2015 for *A. platanoides* and *P. ×hispanica*. While for *A. platanoides* δ^{18}O was significantly elevated in 2004, *P. ×hispanica* showed values significantly lower than average. For *A. platanoides*, δ^{18}O was significantly decreased in 2011 and for *T. cordata* in 2016. For *Q.*

robur δ^{18}O showed no significant deviation from the series mean value in any of the drought years or subsequent years (Fig. 5).

As shown in Fig. 6, across species—but not within species—there was a significant positive relationship between mean δ^{13}C and mean δ^{18}O values ($r = 0.48$, $p = 0.018$). Trees with more positive mean δ^{18}O values showed lower resistance to drought based on the averaged values across the years 2003, 2011 and 2015 ($r = -0.81$, $p < 0.001$). There also existed a slightly negative but non-significant relationship between mean δ^{13}C and mean resistance ($r = -0.39$, $p = 0.058$), such that the wood of trees with higher resistance to drought generally showed lower δ^{13}C values.

Discussion

Influence of weather and particularly drought on stem diameter growth

As expected, we found a number of significant correlations with monthly temperature and precipitation and tree-ring width (TRW) as well as stable isotopes. To our surprise, not only δ^{13}C but especially δ^{18}O showed significant correlations with temperature/precipitation as well as significant deviations from the mean in/after years with drought (Table 2; Fig. 5). As we found a surprisingly good coherence between these general influencing factors on TRW and the effect of drought (timing) on resistance and resilience, we here discuss those results jointly.

The analysis of climate–growth relationships revealed that precipitation in spring is positively correlated with TRW in all of the five species studied (Table 2). As low water availability in spring has a direct effect on the formation of earlywood vessels (Herbette et al. 2010), this is also reflected in the overall TRW. A positive correlation between tree ring growth and precipitation in May has also been found for urban *A. platanoides* trees (Gillner et al. 2014) and for *A. platanoides* and *T. cordata* in forest stands (Fuchs et al. 2021). In those two species, lower precipitation in May is also reflected in less negative δ^{13}C in our study, indicating that the water availability in May is linked to physiological drought stress. Thus, it is not surprising for *A. platanoides* and *T. cordata* to show a particularly low resistance in 2011 (compared to 2003 and 2015)—when the drought period lasted from early spring on and was most severe in May (Fig. 3)—with mean growth levels only reaching 54 % and 64 % of the average growth level of the three preceding

Fig. 6 Correlation between mean values (per tree, $n_{trees} = 6$) of resistance (mean of the years 2003, 2011 and 2015), δ^{13}C and δ^{18}O (mean for 2000–2018)
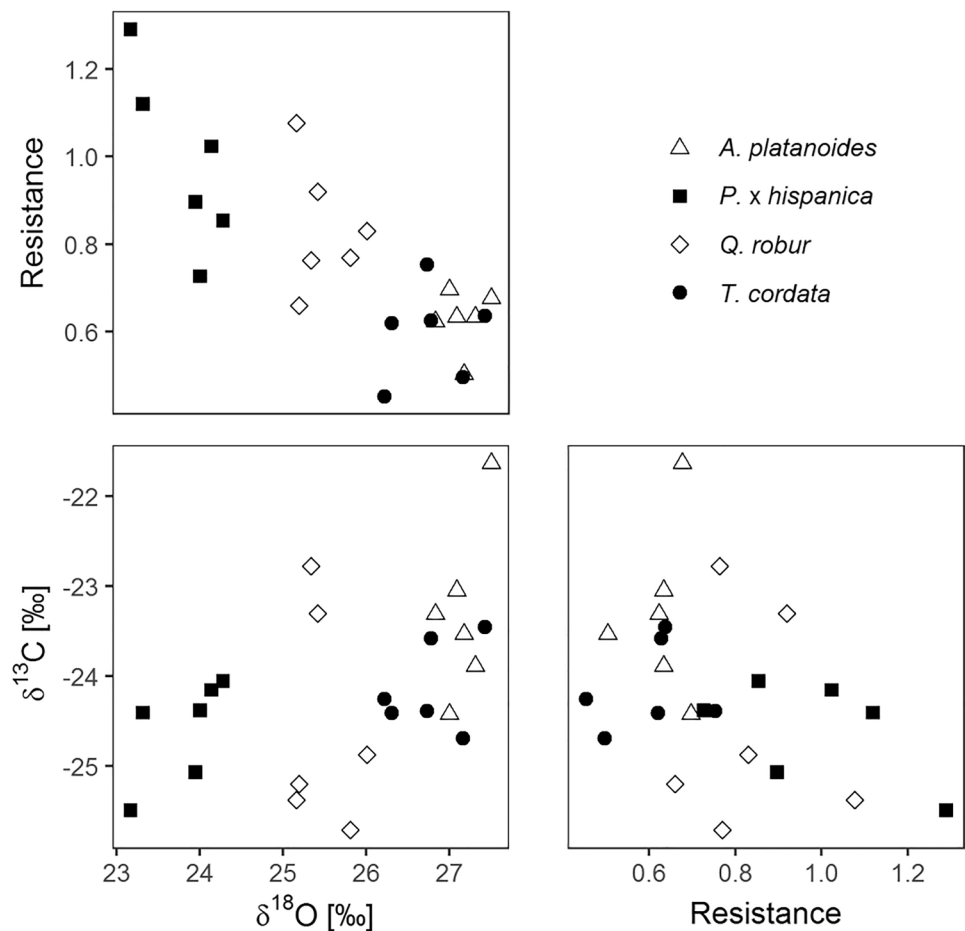
years, respectively (Fig. 4). The severe drought stress in this year is also indicated by significantly elevated $\delta^{13}C$ values (Fig. 5).

Interestingly, there exists a significant negative correlation with May precipitation for $\delta^{18}O$ in all four species, for which isotope analysis were carried out (Table 2). Such negative correlations with precipitation in spring or summer have previously been found for different tree species (Battipaglia et al. 2008; Hartl-Meier et al. 2015). It is difficult to directly translate the oxygen isotope signal in whole wood of tree rings into a physiological response to environmental conditions at the leaf level due to the potential exchange of oxygen in the phloem and during cellulose synthesis (Gessler et al. 2009, 2014; Offermann et al. 2011). Yet, a clear link between precipitation and $\delta^{18}O$ is also indicated when considering the year 2016, where $\delta^{18}O$ values were significantly lower than average in *A. platanoides* and *T. cordata* (Fig. 5). This is probably not a lagged effect of the preceding drought in 2015, but can be explained by unusually high precipitation in this year's spring and early summer, especially June, which received 111 mm of rainfall compared to the long-term average of 76 mm, also reflected by $\delta^{13}C$ values being particularly low in that year in *T. cordata* as well as in *Q. robur* (Fig. 5).

For *Q. robur* TRW was not only positively influenced by precipitation in May/June but also in March (Table 2). Similar relations have been found in *Quercus* spp. for precipitation in March/April and May in urban and forest trees (van der Werf et al. 2007; Gillner et al. 2014; Fuchs et al. 2021). In this ring-porous species, wood formation sets in before bud burst—with a delay between the onset of xylem growth and bud burst of two weeks found in *Q. petraea* in France, where xylem growth began in late March (Michelot et al. 2012), explaining why precipitation before or at the very start of the growing season contributes substantially to the annual diameter growth in this species.

P. × hispanica is the only species for which no significant correlation between precipitation in May and tree ring growth was found, matching the high resistance of this species to the spring drought in 2011, where mean growth reached 94 % of the mean pre-drought growth level. Still, tree ring growth and precipitation in March are positively correlated, similar to *P. × hispanica* trees in Dresden and Szczecin, where higher precipitation in February favoured growth (Cedro and Nowak 2006; Gillner et al. 2014). This species also is the only one to show a positive correlation between tree ring growth and temperature in spring (April), similar to a positive correlation found for the temperature in February in Dresden (Gillner et al. 2014) as well as February and March in Szczecin (Cedro and Nowak 2006), possibly pointing to this species' sensitivity to (late) frost. This may also explain the narrow tree ring

formed in 2013 (Fig. 1), representing the most negative ring width index for this species within the time period 2000–2018. Indeed, in this year, daily minimum temperatures were particularly low for a few days in mid-March and late March (mean of − 6.1 and − 1.8 °C compared to an average of 4.1 and 3 °C, respectively, for the time period 2009–2017). While to our knowledge there are no data available on the leaf phenology of *P. × hispanica* in our study region, we hypothesise that those unusually cold periods may have impacted on bud/leaf development and so shortened the overall length of the growing season and potentially also increased the demand for additional resources (Menzel et al. 2015; Príncipe et al. 2016).

P. × hispanica is also the only species to show a positive relation between the precipitation of the previous summer (June–August) and ring width (Table 2). This lagged effect is also reflected in this species' response to drought. While resistance is not significantly decreased in any of the drought years, average post-drought growth levels only reach ~ 74–85 % of pre-drought growth levels (Fig. 4) and may be indicative of this species' anisohydric response (McDowell et al. 2008; s. below). Thus, while growth is less affected by immediate drought conditions, processes which contribute to growth in the subsequent years are impaired, such as the accumulation of carbohydrates, which are stored for tree ring growth in the subsequent year and show the respective isotope signal (Skomarkova et al. 2006). This may also explain why TRW is negatively correlated with previous year's summer temperature in *A. platanoides* and *C. betulus* (Table 2). In *A. platanoides*, such a lagged effect is indicated by higher $\delta^{13}C$ and $\delta^{18}O$ values occurring in wood formed in years, which were preceded by years with high temperatures in summer (Fig. 5). This can also be seen in 2004 for $\delta^{13}C$ in *Q. robur* and *T. cordata* as well as $\delta^{18}O$ in *A. platanoides*. With the drought in 2003 being most severe in late summer, ring width formation was not substantially affected, as by that time in the year the largest part of the ring had presumably been completed already (Brinkmann et al. 2016; Hentschel et al. 2016), leading to relatively high resistance in most species. Yet, the effect of the drought during the period of carbon assimilation for storage is then visible in the isotopic composition of the following year.

In conclusion, the combined analysis of tree ring width as the overall growth response to the prevailing conditions and of the carbon and oxygen stable isotopes as indicators of physiological drought stress enables a comprehensive interpretation of the effects of temperature and precipitation on tree growth. The importance of May precipitation is indicated by all three variables but especially by the correlation with $\delta^{18}O$ in all species.

Differences between species in the stem diameter growth reaction to drought

Based on the analysis of resistance and resilience we aimed to find out about species-specific drought tolerance. Indeed, irrespective of differences in resistance and resilience between the three years considered, the five species show distinct general patterns of resistance and resilience (Fig. 7), indicating that both immediate and delayed responses to drought have to be taken into account when evaluating the species-specific strategies to cope with drought. To back up those results, we additionally carried out an analysis of the stable carbon and oxygen isotopes. By combining the analysis of the imprint of the physiological response and the resulting stem diameter growth, we expected to gain a deeper insight into the underlying species-specific processes that we will discuss here.

The significantly lower resistance in *A. platanoides* than in the other four species (Fig. 7) indicates that stem growth is substantially impaired by drought in this species, which has also been observed in a study of *Acer* spp., *Quercus* spp. and *P. × hispanica* in the city of Dresden (Gillner et al. 2014). The significantly increased $\delta^{18}O$ in combination with relatively unchanged $\delta^{13}C$ values as observed in 2003 and 2015 (Fig. 5) may, according to the conceptual model of Scheidegger et al. (2000), indicate a decrease in stomatal conductance and photosynthetic capacity—assuming that $\delta^{18}O$ in wood is mostly driven by the variability in stomatal conductance rather than in $\delta^{18}O$ of the source water. Such a response has also been observed in *A. platanoides* during drought in Dresden (Gillner et al. 2015) as well as *A. platanoides* seedlings in a drought experiment (Hommel

et al. 2014). In 2011, however, $\delta^{13}C$ values are significantly increased while $\delta^{18}O$ is significantly lower than average (Fig. 5), which would indicate that photosynthetic capacity increased while stomatal conductance remained unchanged (Scheidegger et al. 2000), as also indicated by the high WUE_i of *A. platanoides* in this year, possibly related to the influence of timing, duration and intensity of drought conditions.

In the above-mentioned study in Dresden, *P. × hispanica* maintained the highest rates for transpiration, stomatal conductance and net photosynthesis during drought of all species studied (Gillner et al. 2015). This may explain why in our study *P. × hispanica* was able to exhibit high resistance to drought—it was the only species without a significant growth reduction compared to the average pre-drought growth levels in any of the three studied drought years (Fig. 4), even though significantly increased $\delta^{18}O$ values in 2003 and 2015 (Fig. 5) may indicate a decrease in stomatal conductance and photosynthetic capacity (Scheidegger et al. 2000), while WUE_i was not affected (Fig. 2).

Q. robur shows slightly lower resistance than *P. × hispanica*, however followed by the highest overall resilience across all species we sampled (Fig. 7). In a young forest stand, *Q. robur* has shown to maintain high transpiration rates despite low precipitation and high evapotranspiration in summer, which can be explained by its deeper rooting system, allowing *Q. robur* to access water in deeper soil layers and so maintain high water potential during drought (Zapater et al. 2012). While it has to be considered that rooting depths of our sample trees may be artificially restricted in urban sites, especially for roadside trees, such a positive effect may still likely explain the overall good performance of *Q. robur* during and after drought, as also indicated by the comparably low mean $\delta^{18}O$ in this species (s. below), especially as none of our sample trees received any artificial irrigation. In ring-porous *Q. robur*, mean growth was neither affected substantially in or after the years 2003 and 2015, in which drought periods occurred in summer, whereas on the contrary both resistance and resilience were especially low in/after 2011 (Fig. 4). This indicates that while TRW of *Q. robur* is largely unaffected by summer drought, spring drought has both an immediate and lasting effect, which is in line with a study of *Q. robur* across Europe (Bose et al. 2021).

T. cordata and *C. betulus* show both comparable resistance and resilience overall, which generally ranges between the values of the other species (Fig. 7). *T. cordata* has been attributed both rather isohydric (Leuschner et al. 2019) and anisohydric behaviour (Gillner et al. 2016; Moser et al. 2017), presumably related to different underlying definitions and traits considered, as well as tree water relations being influenced by environmental factors (Hochberg et al. 2018). In our study, *T. cordata* showed significantly reduced TRW
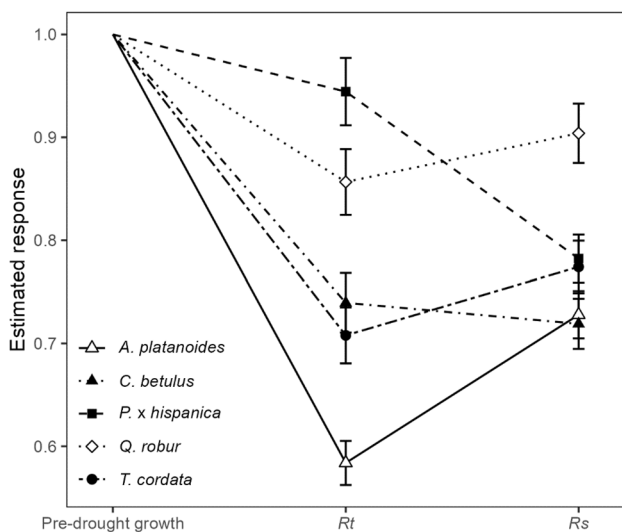

Fig. 7 Estimated marginal means (± standard error) of resistance (*Rt*) and resilience (*Rs*) per species across all years, compared to the mean pre-drought growth level as the relative reference (≙ 100 %)

in 2011 and 2015 (Fig. 4). However, while stem diameter growth may have been reduced or even ceased completely during drought, carbon assimilation may have still been kept up, as it is generally less sensitive to water shortage than xylem growth (Barbaroux and Breda 2002). This is then reflected in elevated $\delta^{13}C$ values in 2011, where the drought occurred during the period of xylem formation, and in 2004, when presumably carbon assimilated during the drought of 2003 was built into the xylem (Fig. 5). After 2015, however, *T. cordata* showed the lowest resilience compared to 2003 and 2011, reaching on average only 69 % of the mean pre-drought growth level after already showing low resistance with a mean growth reduction of 35 % (Fig. 4). This does not necessarily imply reduced drought tolerance but could also be a sign of acclimation to drought (Gessler et al. 2020), especially in combination with *T. cordata* showing enhanced growth of fine roots in deeper soil layers during drought to gain access to further water resources (Stratópoulos et al. 2019).

While *C. betulus* overall showed a similar resistance compared to *T. cordata*, stem diameter growth did generally not recover after the year of the drought, but was on average even lower in the succeeding years, indicating an overall high vulnerability of stem diameter growth to drought (Fig. 7). This species has been found to show a high degree of stomatal regulation upon edaphic/atmospheric drought, probably amplified by its shallow rooting system (Köcher et al. 2009; Zapater et al. 2012). However, *C. betulus* has a comparably cavitation-resistant xylem (Zapater et al. 2012; Li et al. 2016), underlining how the different tree species have developed different strategies to cope with drought.

Concerning the observed differences in the resistance of stem diameter growth to drought between species, the negative correlation between mean tree $\delta^{18}O$ and resistance (Fig. 6) suggests that the inter-specific differences in mean $\delta^{18}O$ may be related to drought tolerance in some way. While it is difficult to disentangle the different processes that affect $\delta^{18}O$ in the xylem (Gessler et al. 2014), the rooting depth could be an important factor, with water in greater soil depths generally being depleted in ^{18}O (Offermann et al. 2011; Gessler et al. 2014; Treydte et al. 2014; Hartl-Meier et al. 2015). Especially, as *P. × hispanica* and *Q. robur,* which show the lowest mean $\delta^{18}O$ values, have higher $d_{1,3}$, tree height and crown size (at time of sampling, Table 1), this could indicate higher belowground biomass and presumably deeper rooting, even though general constraints due to the artificially restricted growing space in our urban study area have to be considered. It appears likely that processes, which influence the species-specific mean $\delta^{18}O$ also affect the species' resistance to drought, even though we cannot determine whether there exists a direct influence (such as greater rooting depth or site conditions) or indirect links between physiological processes, TRW and the oxygen

isotopic composition in wood, and how these are causally connected. For instance, in *T. cordata* a negative correlation between mean $\delta^{18}O$ and the total organic carbon (TOC) of the soil could be observed ($r = -0.78$, $p < 0.001$, $n = 6$). This may indicate that in the mostly sandy soils, the water holding capacity (assumed to be greatly influenced by TOC) has a substantial effect on physiological processes, which is then reflected in the mean isotopic composition of oxygen in wood. However, such a negative correlation did not exist within the other tree species or across species.

Overall, our results are in line with the conclusion of Gillner et al. (2014, 2015), stating that *Acer* spp. is particularly sensitive to drought, while *P. × hispanica* as well as *Quercus* spp. are better suited for urban areas prone to drought. This conclusion is also corroborated by our finding of WUE_i being largely unaffected by drought in *P. × hispanica* and *Q. robur*. However, it also has to be noted that many additional factors have to be considered when evaluating the overall suitability of tree species, such as diseases like the canker stain disease caused by the fungus *Ceratocystis platani*, which has led to the severe dieback of *Platanus* trees throughout North America and Europe (Tsopelas et al. 2017).

Influence of intensity of traffic emissions on the isotopic composition of nitrogen in wood

With our analysis, we aimed to investigate if the isotopic composition of nitrogen can serve as an indicator of traffic emissions in urban trees. Across species, $\delta^{15}N$ values for trees with a maximum distance of 15 m to the next street vary between -2.6 and 10.2 ‰ and are thus well in the range of $\delta^{15}N$ values measured in the air about 10 m from a highway in Switzerland for NO_2 (~ 2–10 ‰) and NO (~ -5 to 10 ‰) by Ammann et al. (1999). A generally large variation in the isotopic composition of nitrogen in roadside air can be explained by a number of factors such as traffic density, the specifications of engines and catalytic converters as well as the mixing of traffic exhaust with ambient air (Ammann et al. 1999; Felix and Elliott 2014). Additionally, it has to be considered that the isotopic composition of wood does not directly reflect that of the air but is also influenced by soil processes and uptake. Especially, the ratio between NH_4 and NO_3 in the soil, which is affected by factors such as an increase in net nitrification due to high nitrogen deposition rates, may influence the $\delta^{15}N$ values of the nitrogen taken up by trees (Hart and Classen 2003; Savard 2010). Most tree species prefer nitrogen uptake as NH_4, which is ^{15}N-enriched, over NO_3, which is ^{15}N-depleted (Hart and Classen 2003), as was confirmed for *C. betulus*, *T. cordata* and *A. pseudoplatanus* growing in a mixed forest stand (Jacob and Leuschner 2014). This contradicts our finding of $\delta^{15}N$ values being significantly lower in *T. cordata* than

in *A. platanoides* and indicates that additional (species-specific) factors such as different rooting depths (Tomlinson et al. 2015) and mycorrhiza (Craine et al. 2009) may play a role as well. A high intensity of colonisation with mycorrhizal fungi of different genera has, for instance, been identified in roadside *T. cordata* trees in Finland (Timonen and Kauppinen 2008). Apart from inter-specific differences, δ^{15}N values are higher in trees located closer to streets and located at sites exposed to higher (estimated) traffic emissions (NO$_x$). Elevated δ^{15}N values in trees closer to roads compared to trees not directly located at the roadside have also been found in *Pinus halepensis* (Mifsud et al. 2021) and *Picea abies* (Saurer et al. 2004; Guerrieri et al. 2009). Hence, we conclude that δ^{15}N values in the wood primarily reflect species-specific nitrogen uptake preferences, rooting depths and mycorrhizal colonisation on the one hand and, to a lesser extent, exposure to NO$_x$ emissions from traffic on the other hand (Table 3). While we did not expect such a strong species-specific variability in nitrogen isotopes, our assumption of δ^{15}N reflecting traffic emissions was confirmed by our analysis. Our analysis thus provides novel insights into the potential use of δ^{15}N as an indicator of NO$_x$ emissions in urban areas, and also the need to account for species-specific variability in the nitrogen isotopic composition of wood. This may however only hold for spatial comparisons with a relatively large sample size as correlations on an annual basis are blurred by radial translocation of nitrogen leading to a certain variability over time, which itself has been shown to not be correlated between trees or with annual nitrogen deposition rates (Hart and Classen 2003).

Influence of site conditions and tree characteristics on intra-specific variability of resistance and resilience to drought

Contrary to our expectations, the resistance and resilience to drought were not influenced by the distance to the nearest street and NO$_x$ emissions from traffic, despite those factors being indicators of NO$_x$ exposition as shown by their significant effects on δ^{15}N in the stem wood. Likewise, a study on trees of the species *Tipuana tipu* in São Paulo showed that growth rates of trees located at sidewalks did not differ significantly from those of trees located in parks (Locosselli et al. 2019), suggesting that growth and drought tolerance of trees in urban areas are not overly influenced by their direct surrounding. Yet, in this mentioned study, trees exposed to higher levels of industrial PM$_{10}$ emissions had lower growth rates than trees being exposed to lower emission levels (Locosselli et al. 2019). In our study area, NO$_x$ and PM$_{10}$ emissions from traffic are highly correlated ($r = 0.89$, $p < 0.001$), so that an effect of PM$_{10}$ could probably not be separated from that of NO$_x$ and would be expected to show as a significant effect of NO$_x$. Additionally, general growth

rates may be affected in a different way than resistance to drought in specific years.

For *T. cordata*, the total organic carbon content of the soil has a positive effect on drought resistance (Table 4). A higher amount of organic carbon in the soil increases water retention, especially in sandy soils (Rawls et al. 2003; Minasny and McBratney 2017)—the soil texture more than 80 % of the sampled *T. cordata* trees grow in. *A. platanoides* was the only species, for which a direct effect of soil texture on resistance could be found (Table 4), pointing to a very specialised requirement regarding soil texture, with a relatively low share of clay, slightly higher share of silt and a considerably high percentage of sand being favourable for the growth of *A. platanoides*, which should however be investigated further. Nonetheless it is interesting to note that those two species, which show comparably strong (physiological) reactions to drought— *A. platanoides* and *T. cordata*—are the only two species whose drought resistance is affected by soil parameters, which are further likely related to the available water capacity of the soil and thus to water supply during drought periods. This finding may also be related to (restricted) root growth in those species, as also indicated by the relatively high mean δ^{18}O values in those two species.

Further, only *T. cordata* trees show a negative effect of tree age on drought resistance, despite maximum age (~ 150 years) in this species being lower than in all other sampled tree species except for *P. × hispanica*. Decreasing resilience with increasing age has also been observed in *Picea abies*, *Abies alba* and *Fagus sylvatica* (Zang et al. 2014), and may be related to reduced photosynthetic activity in older trees, even though the exact mechanisms remain unclear (Yoder et al. 1994; Bond 2000).

In *A. platanoides*, *C. betulus* and *T. cordata* resilience is negatively affected by the pre-drought growth levels (Table 4). This effect of fast-growing trees showing a reduced capacity to return to pre-drought growth levels (in relative terms) has been observed in various tree species (Martinez-Vilalta et al. 2012; Zang et al. 2014). It may be linked to different overall growth strategies, where fast-growing trees allocate proportionally more carbon to aboveground than belowground biomass, which however turns out to be disadvantageous in terms of drought tolerance (Martinez-Vilalta et al. 2012; Zang et al. 2014). Interestingly, those effects can also only be found in those tree species, for which our analysis revealed a generally stronger dependence on water availability, whereas the generally high drought resistance and resilience of *P. × hispanica* and *Q. robur* appear to be largely unaffected by tree or site factors (Table 4). The modelling approach revealed that—within species—resistance to drought is a strong predictor of resilience itself, such that individual trees in which growth was less affected by drought have a higher resilience as well.

However, it has to be noted that this does not imply general intra-specific differences in the vitality of our sample trees, as the ranking of individual trees still differs substantially between years (data not shown).

Altogether, a large part of the intra-specific variability in terms of stem growth reaction to drought remains unexplained (Table 4), indicating that additional factors have to be considered. Studies suggest that the proximity to street lamps (Liu et al. 2021) or mobile phone towers (Waldmann-Selsam et al. 2016) may affect the growth and/or vitality of urban trees. Nonetheless, our results are concomitant with a recent study on hydraulic traits which serve as indicators of drought tolerance—such as the water potential at which xylem conductivity has decreased by 50 % (P_{50})—in *A. platanoides*, *T. cordata* and *C. betulus*, where the greatest part of the variance found in the data could be attributed to individual differences rather than climatic or edaphic conditions (Fuchs et al. 2021). Given such presumed variation in physiological parameters it is not surprising to see intra-specific variability in the resulting growth reactions to drought. In addition, genetic differences may be an important factor as well, especially as we did not take differences between cultivars into account. Last, it has to be considered that due to the complex processes in the soil and between soil and tree, interactions between the measured parameters as well as non-linear effects may occur, so that further studies incorporating those points are needed.

Conclusion

To our knowledge, this is the first study to combine dendroecological and isotope analysis to investigate the drought response of urban trees, especially also considering a potential influence of traffic emissions. Based on our analysis of tree ring widths and the isotopic composition of carbon and oxygen in the whole wood of tree rings, stem diameter growth in the five deciduous tree species is strongly influenced by water availability in spring. Hence, a drought period occurring in spring has a particularly detrimental effect on the current year's stem diameter growth. Physiological drought stress is reflected in elevated $\delta^{13}C$ and/or $\delta^{18}O$ values and increased water-use efficiency in *A. platanoides* and *T. cordata*, which can be concluded to react more sensitively to drought than *Q. robur* and *P. $\times$ hispanica*, while *C. betulus* can be ranked in between concerning its resistance to drought, but shows comparably low resilience. Overall, *Q. robur* exhibits a relatively high resistance and resilience, especially to summer droughts, which may indicate that it is a suitable tree species to be planted in urban areas. With regard to the methods applied, we conclude that neither the analysis of tree ring widths nor stable isotopes alone would have sufficed for the conclusions we drew based on the coupled approach concerning the drought tolerance of urban trees. Further, our study is the first to show that the analysis of $\delta^{15}N$ in the whole wood of the trees can serve as an indicator of the intensity of traffic pollution trees in urban areas are exposed to. However, contrary to our expectations and based on our modelling approach, the respective site conditions such as the amount of NO_x emissions and the distance to the nearest street do not influence resistance and resilience of stem diameter growth to drought. While our study provides valuable knowledge on the suitability of different tree species for urban areas, especially by combining dendroecological and isotope analysis, the trees show a large intra-specific variability, which requires further investigation, especially focussing on physiological processes.

Declarations

References

Ammann M, Siegwolf R, Pichlmayer F, Suter M, Saurer M, Brunold C (1999) Estimating the uptake of traffic-derived NO$_2$ from ^{15}N abundance in Norway spruce needles. Oecologia 118:124–131. https://https://doi.org/10.1007/s004420050710

Barbaroux C, Breda N (2002) Contrasting distribution and seasonal dynamics of carbohydrate reserves in stem wood of adult ring-porous sessile oak and diffuse-porous beech trees. Tree Physiol 22:1201–1210. https://doi.org/10.1093/treephys/22.17.1201

Bates D, Mächler M, Bolker B, Walker S (2015) Fitting linear mixed-effects models using lme4. J Stat Softw 67. https://doi.org/10.18637/jss.v067.i01

Battipaglia G, Jäggi M, Saurer M, Siegwolf RTW, Cotrufo MF (2008) Climatic sensitivity of δ^{18}O in the wood and cellulose of tree rings: Results from a mixed stand of *Acer pseudoplatanus* L. and *Fagus sylvatica* L. Palaeogeogr Palaeoclimatol Palaeoecol 261:193–202. https://doi.org/10.1016/j.palaeo.2008.01.020

Beguería S, Vicente-Serrano SM (2017) SPEI: calculation of the standardised precipitation-evapotranspiration index. R Package Version 1:7

Belmecheri S, Lavergne A (2020) Compiled records of atmospheric CO$_2$ concentrations and stable carbon isotopes to reconstruct climate and derive plant ecophysiological indices from tree rings. Dendrochronologia 63:125748. https://doi.org/10.1016/j.dendro.2020.125748

Ben-Shachar MS, Lüdecke D, Makowski D (2020) effectsize: estimation of effect size indices and standardized parameters. J Open Sour Softw 5:2815

Beyn F, Matthias V, Dahnke K (2014) Changes in atmospheric nitrate deposition in Germany—an isotopic perspective. Environ Pollut 194:1–10. https://doi.org/10.1016/j.envpol.2014.06.043

Bond BJ (2000) Age-related changes in photosynthesis of woody plants. Trends Plant Sci 5:349–353. https://doi.org/10.1016/s1360-1385(00)01691-5

Bose AK, Scherrer D, Camarero JJ, Ziche D, Babst F, Bigler C, Bolte A, Dorado-Liñán I, Etzold S, Fonti P, Forrester DI, Gavinet J, Gazol A, de Andrés EG, Karger DN, Lebourgeois F, Lévesque M, Martínez-Sancho E, Menzel A, Neuwirth B, Nicolas M, Sanders TGM, Scharnweber T, Schröder J, Zweifel R, Gessler A, Rigling A (2021) Climate sensitivity and drought seasonality determine post-drought growth recovery of *Quercus petraea* and *Quercus robur* in Europe. Sci Total Environ. https://doi.org/10.1016/j.scitotenv.2021.147222

Brinkmann N, Eugster W, Zweifel R, Buchmann N, Kahmen A (2016) Temperate tree species show identical response in tree water deficit but different sensitivities in sap flow to summer soil drying. Tree Physiol 36:1508–1519. https://doi.org/10.1093/treephys/tpw062

Bunn A, Korpela M, Biondi F, Campelo F, Mérian P, Qeadan F, Zang C (2021) dplR: dendrochronology program library in R. R Package Version 1(7):2

Cedro A, Nowak G (2006) Effects of climatic conditions on annual tree ring growth of the *Platanus × hispanica* 'Acerifolia' under urban conditions of Szczecin. Dendrobiology 55:11–17

Copernicus land monitoring Service (2021) Urban Atlas LCLU 2018.

Cowling EB, Merrill W (1966) Nitrogen in wood and its role in wood deterioration. Can J Bot 44:1539–1554. https://doi.org/10.1139/b66-167

Craine JM, Elmore AJ, Aidar MP, Bustamante M, Dawson TE, Hobbie EA, Kahmen A, Mack MC, McLauchlan KK, Michelsen A, Nardoto GB, Pardo LH, Penuelas J, Reich PB, Schuur EA, Stock WD, Templer PH, Virginia RA, Welker JM, Wright IJ (2009) Global patterns of foliar nitrogen isotopes and their relationships with climate, mycorrhizal fungi, foliar nutrient concentrations, and nitrogen availability. New Phytol 183:980–992. https://doi.org/10.1111/j.1469-8137.2009.02917.x

Czaja M, Kołton A, Muras P (2020) The complex issue of urban trees—stress factor accumulation and ecological service possibilities. Forests 11:24. https://doi.org/10.3390/f11090932

DIN EN 13657:2003–01 Characterization of waste - Digestion for subsequent determination of aqua regia soluble portion of elements in waste.

DIN EN 15936:2012–11 Sludge, treated biowaste, soil and waste - Determination of total organic carbon (TOC) by dry combustion.

DIN EN ISO 11260:2011–09 Soil quality - Determination of effective cation exchange capacity and base saturation level using barium chloride solution (ISO 11260:1994+Cor. 1:1996).

DIN ISO 11265:1997–06 Soil quality - Determination of the specific electrical conductivity (ISO 11265:1994 + ISO 11265:1994/Corr.1:1996).

Dmuchowski W, Baczewska-Dabrowska A, Gozdowski D, Bragoszewska P, Gworek B, Suwara I, Chojnacki T, Jozwiak A, Swiezewska E (2021) Effect of salt stress in urban conditions on two *Acer* species with different sensitivity. PeerJ 9:e10577. https://doi.org/10.7717/peerj.10577

Dmuchowski W, Brągoszewska P, Gozdowski D, Baczewska-Dąbrowska AH, Chojnacki T, Jozwiak A, Swiezewska E, Suwara I, Gworek B (2020) Strategies of urban trees for mitigating salt stress: a case study of eight plant species. Trees. https://doi.org/10.1007/s00468-020-02044-0

Dobbertin M (2005) Tree growth as indicator of tree vitality and of tree reaction to environmental stress: a review. Eur J Forest Res 124:319–333. https://doi.org/10.1007/s10342-005-0085-3

Dümpelmann S (2020) Urban trees in times of crisis: palliatives, mitigators, and resources. One Earth 2:402–404. https://doi.org/10.1016/j.oneear.2020.04.017

DWD Climate Data Center (CDC) (2020a) Grids of monthly averaged daily air temperature (2 m) over Germany, version v1.0

DWD Climate Data Center (CDC) (2020b) Grids of monthly total precipitation over Germany, version v1.0

Farquhar GD, O'Leary MH, Berry JA (1982) On the relationship between carbon isotope discrimination and the intercellular carbon dioxide concentration in leaves. Funct Plant Biol 9:121–137

Felix JD, Elliott EM (2014) Isotopic composition of passively collected nitrogen dioxide emissions: vehicle, soil and livestock source signatures. Atmos Environ 92:359–366. https://doi.org/10.1016/j.atmosenv.2014.04.005

Fritts HC (1976) Tree rings and climate. Academic Press, London

Fuchs S, Leuschner C, Link RM, Schuldt B (2021) Hydraulic variability of three temperate broadleaf tree species along a water availability gradient in Central Europe. New Phytol. https://doi.org/10.1111/nph.17448

Gessler A, Bottero A, Marshall J, Arend M (2020) The way back: recovery of trees from drought and its implication for acclimation. New Phytol. https://doi.org/10.1111/nph.16703

Gessler A, Brandes E, Buchmann N, Helle G, Rennenberg H, Barnard RL (2009) Tracing carbon and oxygen isotope signals from newly assimilated sugars in the leaves to the tree-ring archive. Plant Cell Environ 32:780–795. https://doi.org/10.1111/j.1365-3040.2009.01957.x

Gessler A, Cailleret M, Joseph J, Schönbeck L, Schaub M, Lehmann M, Treydte K, Rigling A, Timofeeva G, Saurer M (2018) Drought induced tree mortality—a tree-ring isotope based conceptual model to assess mechanisms and predispositions. New Phytol 219:485–490. https://doi.org/10.1111/nph.15154

Gessler A, Ferrio JP, Hommel R, Treydte K, Werner RA, Monson RK (2014) Stable isotopes in tree rings: towards a mechanistic

understanding of isotope fractionation and mixing processes from the leaves to the wood. Tree Physiol 34:796–818. https://doi.org/10.1093/treephys/tpu040

Gillner S, Bräuning A, Roloff A (2014) Dendrochronological analysis of urban trees: climatic response and impact of drought on frequently used tree species. Trees 28:1079–1093. https://doi.org/10.1007/s00468-014-1019-9

Gillner S, Korn S, Hofmann M, Roloff A (2016) Contrasting strategies for tree species to cope with heat and dry conditions at urban sites. Urban Ecosyst 20:853–865. https://doi.org/10.1007/s11252-016-0636-z

Gillner S, Korn S, Roloff A (2015) Leaf-gas exchange of five tree species at urban stree sites. Arboricult Urban for 41:113–124

Grömping U (2006) Relative importance for linear regression in R: The Package relaimpo. J Stat Softw 17. https://doi.org/10.18637/jss.v017.i01

Grömping U (2015) Variable importance in regression models. Wiley Interdisciplinary Rev Comput Stat 7:137–152. https://doi.org/10.1002/wics.1346

Grote R, Samson R, Alonso R, Amorim JH, Cariñanos P, Churkina G, Fares S, Thiec DL, Niinemets Ü, Mikkelsen TN, Paoletti E, Tiwary A, Calfapietra C (2016) Functional traits of urban trees: air pollution mitigation potential. Front Ecol Environ 14:543–550. https://doi.org/10.1002/fee.1426

Guerrieri MR, Siegwolf RTW, Saurer M, Jäggi M, Cherubini P, Ripullone F, Borghetti M (2009) Impact of different nitrogen emission sources on tree physiology as assessed by a triple stable isotope approach. Atmos Environ 43:410–418. https://doi.org/10.1016/j.atmosenv.2008.08.042

Hart SC, Classen AT (2003) Potential for assessing long-term dynamics in soil nitrogen availability from variations in $\delta^{15}N$ of tree rings. Isotopes Environ Health Stud 39:15–28. https://doi.org/10.1080/1025601031000102206

Hartl-Meier C, Zang C, Buntgen U, Esper J, Rothe A, Gottlein A, Dirnbock T, Treydte K (2015) Uniform climate sensitivity in tree-ring stable isotopes across species and sites in a mid-latitude temperate forest. Tree Physiol 35:4–15. https://doi.org/10.1093/treephys/tpu096

Helama S, Läänelaid A, Raisio J, Sohar K, Mäkelä A (2020) Growth patterns of roadside *Tilia* spp. affected by climate and street maintenance in Helsinki. Urban For Urban Green 53:126707. https://doi.org/10.1016/j.ufug.2020.126707

Hentschel R, Hommel R, Poschenrieder W, Grote R, Holst J, Biernath C, Gessler A, Priesack E (2016) Stomatal conductance and intrinsic water use efficiency in the drought year 2003: a case study of European beech. Trees 30:153–174. https://doi.org/10.1007/s00468-015-1284-2

Herbette S, Wortemann R, Awad H, Huc R, Cochard H, Barigah TS (2010) Insights into xylem vulnerability to cavitation in *Fagus sylvatica* L.: phenotypic and environmental sources of variability. Tree Physiol 30:1448–1455. https://doi.org/10.1093/treephys/tpq079

Hochberg U, Rockwell FE, Holbrook NM, Cochard H (2018) Iso/Anisohydry: a plant-environment interaction rather than a simple hydraulic trait. Trends Plant Sci 23:112–120. https://doi.org/10.1016/j.tplants.2017.11.002

Hofman J, Wuyts K, Van Wittenberghe S, Samson R (2014) On the temporal variation of leaf magnetic parameters: seasonal accumulation of leaf-deposited and leaf-encapsulated particles of a roadside tree crown. Sci Total Environ 493:766–772. https://doi.org/10.1016/j.scitotenv.2014.06.074

Hommel R, Siegwolf R, Saurer M, Farquhar GD, Kayler Z, Ferrio JP, Gessler A (2014) Drought response of mesophyll conductance in forest understory species—impacts on water-use efficiency and interactions with leaf water movement. Physiol Plant 152:98–114. https://doi.org/10.1111/ppl.12160

Hyndman RJ, G. A, Bergmeir C, Caceres G, Chhay L, O'Hara-Wild M, F. P, Razbash S, Wang E, Yasmeen F, (2021) forecast: forecasting functions for time series and linear models. R Package Version 8:15

Jacob A, Leuschner C (2014) Complementarity in the use of nitrogen forms in a temperate broad-leaved mixed forest. Plant Ecolog Divers 8:243–258. https://doi.org/10.1080/17550874.2014.898166

Jeanjean APR, Gallagher J, Monks PS, Leigh RJ (2017) Ranking current and prospective NO$_2$ pollution mitigation strategies: an environmental and economic modelling investigation in Oxford Street, London. Environ Pollut 225:587–597. https://doi.org/10.1016/j.envpol.2017.03.027

Kändler G, Adler P, Hellbach A (2011) Konzept zur Erfassung der Kohlenstoff-Speicherleistung von Stadtbäumen am Beispiel der Stadt Karlsruhe. Forstliche Versuchs- und Forschungsanstalt Baden-Württemberg, Freiburg

Keeling CD, Piper SC, Bacastow RB, Wahlen M, Whorf TP, Heimann M, Meijer HA (2005) Atmospheric CO$_2$ and $^{13}CO_2$ exchange with the terrestrial biosphere and oceans from 1978 to 2000: observations and carbon cycle implications. In: Ehleringer JR, Cerling TE, Dearing MD (eds) A history of atmospheric CO$_2$ and its effects on plants, animals, and ecosystems. Springer Verlag, New York, pp 83–113

Keeling RF, Keeling CD (2017) Atmospheric Monthly In Situ CO2 Data-Mauna Loa Observatory, Hawaii. In Scripps CO2 Program Data. UC San Diego Library Digital Collections. https://doi.org/10.6075/J08W3BH

Köcher P, Gebauer T, Horna V, Leuschner C (2009) Leaf water status and stem xylem flux in relation to soil drought in five temperate broad-leaved tree species with contrasting water use strategies. Ann Sci 66:101–101. https://doi.org/10.1051/forest/2008076

Kuznetsova A, Brockhoff PB, Christensen RHB (2017) lmerTest package: Tests in linear mixed effects models. J Stat Softw 82:1–26

Lenth RV (2021) emmeans: Estimated marginal means, aka least-squares means. R Package Version 1(5):4

Leuschner C, Wedde P, Lübbe T (2019) The relation between pressure–volume curve traits and stomatal regulation of water potential in five temperate broadleaf tree species. Ann Sci. https://doi.org/10.1007/s13595-019-0838-7

Li S, Feifel M, Karimi Z, Schuldt B, Choat B, Jansen S (2016) Leaf gas exchange performance and the lethal water potential of five European species during drought. Tree Physiol 36:179–192. https://doi.org/10.1093/treephys/tpv117

Liu P, Cao B, Wang Y, Wei Z, Ye J, Wei H (2021) Spectral effect of streetlamps on urban trees: a simulated study on tissue water, nitrogen, and carbohydrate contents in maple and oak. PLoS ONE 16:e0248463. https://doi.org/10.1371/journal.pone.0248463

Lloret F, Keeling EG, Sala A (2011) Components of tree resilience: effects of successive low-growth episodes in old ponderosa pine forests. Oikos 120:1909–1920. https://doi.org/10.1111/j.1600-0706.2011.19372.x

Locosselli GM, Camargo EP, Moreira TCL, Todesco E, Andrade MF, Andre CDS, Andre PA, Singer JM, Ferreira LS, Saldiva PHN, Buckeridge MS (2019) The role of air pollution and climate on the growth of urban trees. Sci Total Environ 666:652–661. https://doi.org/10.1016/j.scitotenv.2019.02.291

LUBW (2013) Zukünftige Klimaentwicklung in Baden-Württemberg. Perspektiven aus regionalen Klimamodellen. Langfassung. Karlsruhe

LUBW (2014) Flächendeckende Ermittlung der Immissions-Vorbelastung für Baden-Württemberg 2010. Ausbreitungsrechnungen unter Verwendung des landesweiten Emissionskatasters und unter Berücksichtigung von gemessenen Immissionsdaten.

LUBW (2017) Luftschadstoff-Emissionskataster Baden-Württemberg 2014.

Maher BA, Ahmed IA, Davison B, Karloukovski V, Clarke R (2013) Impact of roadside tree lines on indoor concentrations of traffic-derived particulate matter. Environ Sci Technol 47:13737–13744. https://doi.org/10.1021/es404363m

Martinez-Vilalta J, Lopez BC, Loepfe L, Lloret F (2012) Stand- and tree-level determinants of the drought response of Scots pine radial growth. Oecologia 168:877–888. https://doi.org/10.1007/s00442-011-2132-8

McCarroll D, Loader NJ (2004) Stable isotopes in tree rings. Quatern Sci Rev 23:771–801. https://doi.org/10.1016/j.quascirev.2003.06.017

McDowell N, Pockman WT, Allen CD, Breshears DD, Cobb N, Kolb T, Plaut J, Sperry J, West A, Williams DG, Yepez EA (2008) Mechanisms of plant survival and mortality during drought: why do some plants survive while others succumb to drought? New Phytol 178:719–739. https://doi.org/10.1111/j.1469-8137.2008.02436.x

Menzel A, Helm R, Zang C (2015) Patterns of late spring frost leaf damage and recovery in a European beech (*Fagus sylvatica* L.) stand in south-eastern Germany based on repeated digital photographs. Front Plant Sci 6:110. https://doi.org/10.3389/fpls.2015.00110

Michelot A, Simard S, Rathgeber C, Dufrene E, Damesin C (2012) Comparing the intra-annual wood formation of three European species (*Fagus sylvatica*, *Quercus petraea* and *Pinus sylvestris*) as related to leaf phenology and non-structural carbohydrate dynamics. Tree Physiol 32:1033–1045. https://doi.org/10.1093/treephys/tps052

Mifsud DV, Stueken EE, Wilson RJS (2021) A preliminary study into the use of tree-ring and foliar geochemistry as bio-indicators for vehicular NO_x pollution in Malta. Isotopes Environ Health Stud 1–15. https://doi.org/10.1080/10256016.2021.1902319

Millard P, Grelet GA (2010) Nitrogen storage and remobilization by trees: Ecophysiological relevance in a changing world. Tree Physiol 30:1083–1095. https://doi.org/10.1093/treephys/tpq042

Minasny B, McBratney AB (2017) Limited effect of organic matter on soil available water capacity. Eur J Soil Sci 69:39–47. https://doi.org/10.1111/ejss.12475

Moser A, Rahman MA, Pretzsch H, Pauleit S, Rotzer T (2017) Inter- and intraannual growth patterns of urban small-leaved lime (*Tilia cordata* mill.) at two public squares with contrasting microclimatic conditions. Int J Biometeorol 61:1095–1107. https://doi.org/10.1007/s00484-016-1290-0

Müller-Haubold H, Hertel D, Seidel D, Knutzen F, Leuschner C (2013) Climate responses of aboveground productivity and allocation in *Fagus sylvatica*: a transect study in mature forests. Ecosystems 16:1498–1516. https://doi.org/10.1007/s10021-013-9698-4

Mund M, Kutsch WL, Wirth C, Kahl T, Knohl A, Skomarkova MV, Schulze ED (2010) The influence of climate and fructification on the inter-annual variability of stem growth and net primary productivity in an old-growth, mixed beech forest. Tree Physiol 30:689–704. https://doi.org/10.1093/treephys/tpq027

Offermann C, Ferrio JP, Holst J, Grote R, Siegwolf R, Kayler Z, Gessler A (2011) The long way down—are carbon and oxygen isotope signals in the tree ring uncoupled from canopy physiological processes? Tree Physiol 31:1088–1102. https://doi.org/10.1093/treephys/tpr093

OpenStreetMap contributors (2021)

Pace R, De Fino F, Rahman MA, Pauleit S, Nowak DJ, Grote R (2020) A single tree model to consistently simulate cooling, shading, and pollution uptake of urban trees. Int J Biometeorol. https://doi.org/10.1007/s00484-020-02030-8

Príncipe A, van der Maaten E, van der Maaten-Theunissen M, Struwe T, Wilmking M, Kreyling J (2016) Low resistance but high resilience in growth of a major deciduous forest tree (*Fagus sylvatica* L.) in response to late spring frost in southern Germany. Trees 31:743–751. https://doi.org/10.1007/s00468-016-1505-3

QGIS.org (2021) QGIS Geographic Information System. QGIS Association. http://www.qgis.org.

R Core Team (2020) R: A language and environment for statistical computing. R Foundation for Statistical Computing, Vienna, Austria

Rawls WJ, Pachepsky YA, Ritchie JC, Sobecki TM, Bloodworth H (2003) Effect of soil organic carbon on soil water retention. Geoderma 116:61–76. https://doi.org/10.1016/s0016-7061(03)00094-6

Richter S, Haase D, Thestorf K, Makki M (2020) Carbon pools of Berlin, Germany: organic carbon in soils and aboveground in trees. Urban for Urban Green 54:126777. https://doi.org/10.1016/j.ufug.2020.126777

Roden J, Siegwolf R (2012) Is the dual-isotope conceptual model fully operational? Tree Physiol 32:1179–1182. https://doi.org/10.1093/treephys/tps099

Sanusi R, Livesley SJ (2020) London Plane trees (*Platanus* x *acerifolia*) before, during and after a heatwave: LOSING leaves means less cooling benefit. Urban for Urban Green 54:126746. https://doi.org/10.1016/j.ufug.2020.126746

Saurer M, Cherubini P, Ammann M, De Cinti B, Siegwolf R (2004) First detection of nitrogen from NO_x in tree rings: a $^{15}N/^{14}N$ study near a motorway. Atmos Environ 38:2779–2787. https://doi.org/10.1016/j.atmosenv.2004.02.037

Savard MM (2010) Tree-ring stable isotopes and historical perspectives on pollution—an overview. Environ Pollut 158:2007–2013. https://doi.org/10.1016/j.envpol.2009.11.031

Scheidegger Y, Saurer M, Bahn M, Siegwolf R (2000) Linking stable oxygen and carbon isotopes with stomatal conductance and photosynthetic capacity: a conceptual model. Oecologia 125:350–357. https://doi.org/10.1007/s004420000466

Skomarkova MV, Vaganov EA, Mund M, Knohl A, Linke P, Boerner A, Schulze ED (2006) Inter-annual and seasonal variability of radial growth, wood density and carbon isotope ratios in tree rings of beech (*Fagus sylvatica*) growing in Germany and Italy. Trees 20:571–586. https://doi.org/10.1007/s00468-006-0072-4

Spiecker H, Schinker MG, Hansen J, Park Y-I, Ebding T, Döll W (2000) Cell structure in tree rings: Novel methods for preparation and image analysis of large cross sections. IAWA J 21:361–373

Stratópoulos LMF, Zhang C, Duthweiler S, Haberle KH, Rotzer T, Xu C, Pauleit S (2019) Tree species from two contrasting habitats for use in harsh urban environments respond differently to extreme drought. Int J Biometeorol 63:197–208. https://doi.org/10.1007/s00484-018-1653-9

Strohbach MW, Haase D (2012) Above-ground carbon storage by urban trees in Leipzig, Germany: analysis of patterns in a European city. Landsc Urban Plan 104:95–104. https://doi.org/10.1016/j.landurbplan.2011.10.001

Timonen S, Kauppinen P (2008) Mycorrhizal colonisation patterns of Tilia trees in street, nursery and forest habitats in southern Finland. Urban for Urban Green 7:265–276. https://doi.org/10.1016/j.ufug.2008.08.001

Tomlinson G, Buchmann N, Siegwolf R, Weber P, Thimonier A, Pannatier EG, Schmitt M, Schaub M, Waldner P (2015) Can tree-ring $\delta^{15}N$ be used as a proxy for foliar $\delta^{15}N$ in European beech and Norway spruce? Trees 30:627–638. https://doi.org/10.1007/s00468-015-1305-1

Treydte K, Boda S, Graf Pannatier E, Fonti P, Frank D, Ullrich B, Saurer M, Siegwolf R, Battipaglia G, Werner W, Gessler A (2014) Seasonal transfer of oxygen isotopes from precipitation and soil to the tree ring: source water versus needle water enrichment. New Phytol 202:772–783. https://doi.org/10.1111/nph.12741

Tsopelas P, Santini A, Wingfield MJ, Wilhelm de Beer Z (2017) Canker stain: a lethal disease destroying iconic plane trees. Plant Dis 101:645–658. https://doi.org/10.1094/PDIS-09-16-1235-FE

van der Maaten-Theunissen M, van der Maaten E, Bouriaud O (2015) pointRes: An R package to analyze pointer years and components of resilience. Dendrochronologia 35:34–38. https://doi.org/10.1016/j.dendro.2015.05.006

van der Werf GW, Sass-Klaassen UGW, Mohren GMJ (2007) The impact of the 2003 summer drought on the intra-annual growth pattern of beech (*Fagus sylvatica* L.) and oak (*Quercus robur* L.) on a dry site in the Netherlands. Dendrochronologia 25:103–112. https://doi.org/10.1016/j.dendro.2007.03.004

VDLUFA (1991) Methodenbuch, vol 1. VDLUFA-Verlag, Darmstadt, Die Untersuchung von Böden

Vitali V, Klesse S, Weigt R, Treydte K, Frank D, Saurer M, Siegwolf RTW (2021) High-frequency stable isotope signals in uneven-aged forests as proxy for physiological responses to climate in Central Europe. Tree Physiol 41:2046–2062. https://doi.org/10.1093/treephys/tpab062

Waldmann-Selsam C, Balmori-de la Puente A, Breunig H, Balmori A (2016) Radiofrequency radiation injures trees around mobile phone base stations. Sci Total Environ 572:554–569. https://doi.org/10.1016/j.scitotenv.2016.08.045

Waring RH (1987) Characteristics of trees predisposed to die. Bioscience 37:569–574. https://doi.org/10.2307/1310667

Yoder BJ, Ryan MG, Waring RH, Schoettle AW, Kaufmann MR (1994) Evidence of reduced photosynthetic rates in old trees. For Sci 40:513–527. https://doi.org/10.1093/forestscience/40.3.513

Zacharias S, Koppe C, Mücke H-G (2014) Climate change effects on heat waves and future heat wave-associated IHD mortality in Germany. Climate 3:100–117. https://doi.org/10.3390/cli3010100

Zang C, Biondi F (2015) treeclim: an R package for the numerical calibration of proxy-climate relationships. Ecography 38:431–436. https://doi.org/10.1111/ecog.01335

Zang C, Hartl-Meier C, Dittmar C, Rothe A, Menzel A (2014) Patterns of drought tolerance in major European temperate forest trees: climatic drivers and levels of variability. Glob Chang Biol 20:3767–3779. https://doi.org/10.1111/gcb.12637

Zapater M, Bréda N, Bonal D, Pardonnet S, Granier A (2012) Differential response to soil drought among co-occurring broad-leaved tree species growing in a 15- to 25-year-old mixed stand. Ann Sci 70:31–39. https://doi.org/10.1007/s13595-012-0233-0

Zhang C, Stratopoulus LMF, Pretzsch H, Rötzer T (2019) How do *Tilia cordata* greenspire trees cope with drought stress regarding their biomass allocation and ecosystem services? Forests 10

Publisher's Note Springer Nature remains neutral with regard to jurisdictional claims in published maps and institutional affiliations.